MSDE

REVIEW

View Article Online
View Journal | View Issue

Cite this: *Mol. Syst. Des. Eng.*, 2023, **8**, 560

Metal–organic framework composites from a mechanochemical process

Wupeng Wang,[a] Milton Chai,*[a] Muhammad Yazid Bin Zulkifli,[b] Kaijie Xu,[a] Yuelei Chen,[a] Lianzhou Wang,[a] Vicki Chen[b] and Jingwei Hou*[a]

Received 10th October 2022,
Accepted 19th December 2022

DOI: 10.1039/d2me00211f

rsc.li/molecular-engineering

Metal–organic frameworks (MOFs) consist of metal ions or clusters coordinated with organic ligands such as imidazolate or carboxylate ligands. Owing to the high porosity and surface area of MOFs, researchers have applied MOFs as host matrixes for other functional materials to form MOF composites with improved stability and functionality. The current research focus is mainly on solution-based synthesis, such as infiltration synthesis and template synthesis. Mechanochemistry has not been explored much toward MOF composites. This review will discuss the current progress on mechanochemically synthesized MOF composites and their strengths and weaknesses as compared with the traditional solution-based methods. The review will also cover the importance of mechanochemistry and the fundamentals behind it, such as interfacial interaction and milling impact factors. Furthermore, the applications of mechanochemically synthesized composites are highlighted, including catalysis, adsorption, energy generation, and storage.

Design, System, Application

Mechanochemistry utilize mechanical energy generated by compression, shearing, and grinding to achieve fast, facile, and green chemical synthesis and have already been applied in many fields. Furthermore, mechanochemical synthesis is more time-efficient and cost-effective compared to traditional solution-based methods. Large production is also feasible. Owing to the high porosity, surface area, and stability of MOFs, they could be employed as host matrixes to embed other functional materials, such as perovskite and metal nanoparticles, particularly *via* the mechanochemical process. However, without a complete picture of the mechanism, it is hard to precisely control the synthesis process. More detailed *in situ* monitoring is urgently needed. Moreover, interfacial property is an important aspect for composites. For example, compositing two types of crystalline MOF needs careful consideration of their lattice matching/mismatching. MOF glass, also known as "frozen MOF liquid", is a recently emerging research area. Owing to the relatively higher entropy (and therefore energy) of MOF glass compared to its MOF crystal, glass can have better processability and compatibility with the secondary components, which enables a whole array of composites, particularly *via* the mechanochemical process.

Introduction

Mechanochemical synthesis refers to chemical formation and reaction sustained by mechanical factors, including shearing, compression, and grinding (Fig. 1).[3] By initializing chemical synthesis *via* mechanical action, this route is usually considered as green synthesis because it is solvent free or only requires only a little amount of solvent, which could mitigate environmental impact on solvent disposal. Apart from this, it could also provide other advantages such as short reaction time,[4–6] high conversion efficiency,[7,8] and opens up new pathways that would otherwise be difficult to fill with other synthetic methods.[9] Due to these unique advantages, mechanochemical synthesis has been regarded as one of the top 10 world-changing chemistry innovations[10] and has been dubbed as chemical 2.0.

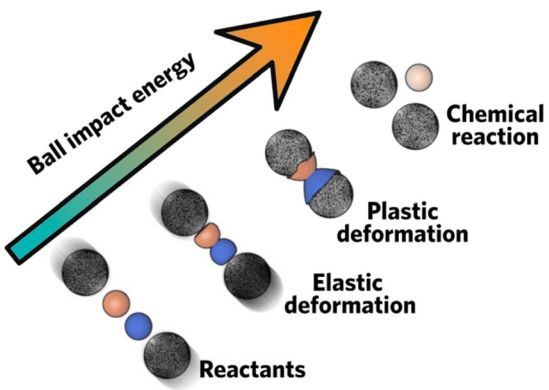

Fig. 1 Schematic procedures of mechanochemical ball milling. Reproduced with permission from ref. 3.

[a] School of Chemical Engineering, The University of Queensland, Australia.
E-mail: milton.chai@uq.edu.au, jingwei.hou@uq.edu.au
[b] School of Chemical Engineering, The University of New South Wales, Australia

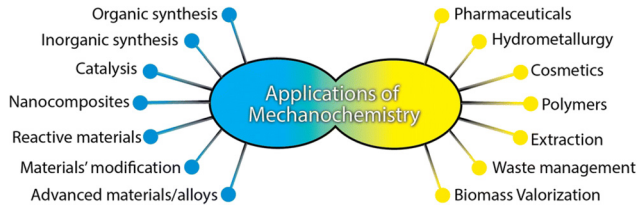

Fig. 2 Application of mechanochemistry. Reproduced with permission from ref. 13.

Mechanochemical synthesis has a long history and can be dated back to prehistoric times, when Theophrastus in his book entitled "On Stones" recorded people using copper-made mortar and pestle to grind cinnabar (HgS) to get elemental mercury.[11] In the 19th century, the research on mechanochemical synthesis started to emerge, for example, Faraday in 1820 described his "dry way" reaction, which is the reduction of silver chloride by grinding zinc, tin, iron, and copper in a mortar with pestle.[11] The term "mechanochemistry" was first introduced by Wilhelm Ostwald in the "Textbook of General Chemistry" in 1891 and IUPAC (International Union of Pure and Applied Chemistry), which defined the term "mechanochemical reaction" as "a chemical reaction that is induced by the direct absorption of mechanical energy".[12] To date, mechanochemical synthesis has already been used in many fields, and Fig. 2 summarizes the most common fields where mechanochemistry has been applied.[13]

Hand grinding (Fig. 3a) is the first approach of mechanochemical synthesis and generally uses a mortar and pestle, which is the easiest and most straightforward way to generate mechanical energy. This process, however, can be difficult to control and reproduce, and is usually affected by environmental factors such as moisture and temperature. With technological development, machine-based milling tools are used more, such as a planetary miller (Fig. 3b–i),[14,15] which generally refers to the ball milling process. During ball milling, the reactants are crushed by balls, generating mechanical energy. This process provides the energy needed for chemical reaction, such as bond breakage and formation. Meanwhile, continuous ball milling process ensure continuous exposure of active sites on the reactants surface, which facilitate the reaction process. As the milling reaction mainly happens at the interface between the phases, it is necessary to create a large surface area for better reaction, which can be tuned by reaction conditions such as ball size and milling time.[16] Mechanical milling can generate much higher and sustained energy compared to hand milling and provide inert reaction conditions by flowing inert gas. It should be noted that an excessive amount of mechanical energy might destroy the material structure and lead to amorphization. In addition, a small amount of solvent could also be added during milling to optimize and control the milling condition.[17]

Fig. 3 Commonly used milling equipment. (a) Mortar and pestle, (b) automatic mortar, (c) vertical vibrational mini mill, (d) vibratory micro-mill, (e) vibrational ball mill, (f) vibrational ball mill with temperature control, (g) planetary ball mill, (h) multisampling mill, and (i) twin-screw for continuous mechanochemical synthesis. Reproduced with permission from ref. 15.

Current focuses on MOFs are on tuning the MOFs structure and exploring new applications[18–20] owing to the vast available functional group and sub-families of MOFs. Their rich chemistry and structure also enable the development of MOF composites through the combination of MOFs with one or more other functional materials. In the composite material, the advantages of both MOFs, such as high porosity, structure flexibility, and adaptivity, and the hosted functional material, including optical,[21] electrical,[22] magnetic,[23] and catalytic[24] properties, could be combined, thus providing unique chemical and physical properties of the formed MOF composite. In addition, most MOF materials are synthesized as discrete powders, imposing significant challenge in their device assembly.[25] As a result, these fields of study have been rapidly evolving recently, particularly in combination with mechanochemistry.

Current review papers on the MOF composite mainly focus on the integrated functional groups and their applications, such as enzymes[26] and nanoparticles,[27] with infiltration and template methods being the main reported methods. Although these papers briefly mention mechanochemistry in the MOF composite, they still lack research on mechanochemical composting principles. This review paper will not only review the mechanochemical synthesized MOF composite, including how they are synthesized, what has been achieved, and their benefits compared to the conventional method, but also discuss the mechanochemical composting principles and scientific factors behind it. We hope that this will shed light on the process and guide future research in this area.

Conventional strategies to synthesize MOF composites

Traditionally, there are broader techniques to construct a MOF composite, taking advantage of their large surface area and framework structures, namely, "ship-in-bottle" and "bottle-around-ship". Ship-in-bottle synthesis refers to introducing guest molecules or guest precursors into the MOF pores. Infiltration method either *via* solution or gas is the most commonly used strategy to synthesize such MOF composites.

The solution infiltration method uses the porosity and capillary force of the MOFs in the solution. Prior to the solution infiltration process, the solvents in the MOF pores are removed through an activation process that may involve the exchange of a high boiling point solvent with a low boiling point solvent, followed by heating to obtain an empty framework. Subsequently, the desolvated porous MOFs are soaked in the solution for infiltration, such as metal salts solution, followed by *in situ* reaction to form the guest components. For example, to form the Pd/MIL-100 ($Al_3O(OH)(H_2O)_2[btc]_2{\cdot}nH_2O$) composites, activated MIL-100 powder was mixed with tetrachloropalladinic acid solution (H_2PdCl_4) and stirred for 3 h, followed by hydrogen reduction in air/H_2 flow at 553 K for 6 h and vacuum drying.[28]

Gas phase infiltration, also called chemical vapor deposition, one of the early pioneer experiments, was performed by Fischer and co-workers.[29] They exposed desolvated MOF-5 ($Zn_4O(BDC)_3$, where BDC = 1,4-benzodicarboxylate) to the metal precursor vapor instead of solution in a sealed vacuum Schlenk tube. By changing the temperature based on the vapor pressure, the precursors were successfully trapped inside the MOF pores. Further treatment is still needed to get the desired MOF composite, such as treating with hydrogen reduction or thermal decomposition to get metal-embedded MOF composite.

Both these infiltration methods face difficulties in introducing precursors inside the MOF's narrow pores.[30] Therefore, the formed nanoparticles are usually found on the external surface of the composites MOFs, resulting in low stability.[31] A double solvent method has been developed to solve the above problem by dissolving both metal precursors (H_2PtCl_6) and a hydrophobic solvent (hexane) to suspend the absorption on the external surface and facilitate the impregnation inside the pores.[32] However, this method consumed additional solvent and time.

The bottle-around-ship method, on the other hand, involves synthesizing the functional nanoparticles first, and then crystallizing MOFs around the nanoparticles. Templated synthesis is the most common method used for bottle-around-ship synthesis by binding nanoparticles on the desired MOFs' metal source or ligands with the help of surfactants or capping agents. The addition of surfactants not only stabilizes nanoparticles in the solution but also facilitates the growth of MOFs due to coordination interactions between the surfactants and metal ions of MOFs.[33] Even though much efforts have been made for developing this strategy, it is not as facile and convenient compared to infiltration methods. For example, surfactants are usually organic materials, which are relatively hard to remove; therefore, the active site might be captured by the remaining surfactants and hinder their applications.[31] Nevertheless, template synthesis also has some strengths. For example, Lu *et al.* found that the spatial distribution of metal nanoparticles within ZIF-8 ($[Zn(mIm)_2]$, where mIm = 2-methylimidazole) crystals could be controlled by varying the time of nanoparticle addition during the synthesis of the MOF.[33]

MOF synthesis by conventional solution methods usually have weak mechanical properties caused by the trade-off between porosity and mechanical properties,[34,35] which hamper composite application in absorption and separation processes.[36] Despite the efforts made to solve the problem,[37–40] MOF aggregation and unsatisfactory mechanical properties are still inevitable, which limits the composite application. Meanwhile, pore aperture size is another factor that impacts the formation of the composite. If a guest molecule is too large for the pore, it is hard to form composites by absorbing them into the pore during infiltration. In light of this, mechanochemical synthesis is another viable synthesis method that can be implemented, which has yet to be researched in detail. Considering the nature of mechanochemical synthesis, it could provide fast and facile synthesis without using a large amount of solvent, which brings both economic and environmental benefits. Meanwhile, mechanochemically synthesized MOF composite enables faster and more controllable routes compared with other solution-based methods. It also does not require high temperature treatment to introduce crystallization, which makes it friendly to some thermally-sensitive secondary materials, such as enzymes.[24] In addition, large-scale synthesis is also feasible *via* the mechanochemical method, which allows for their implementation at an industrial scale.

Mechanochemistry

Brief fundamentals of mechanochemical synthesis

Similar to all other material synthesis techniques, the mechanochemical process offers a high dimensional parameter space for process control and optimization. The milling parameters, including milling types, materials, size, time, temperature, atmosphere, rotation speed, frequency, ball/powder weight ratio, filling ratio, and process control agents, could impact the final products and their properties.[41] Compared to the solution-based method, mechanochemical synthesis could reduce the particle size and increase the pore and surface area.

Many mechanochemical works convert the energy to local heat; hence, some scientists claim that mechanochemical synthesis is the result of local heating instead of chemical deformation.[11] Many evidences have shown that even though mechanochemistry has been developed for such a long time, the understanding of the underlying mechanism is relatively limited. To better control the mechanochemical synthesis process, a deeper and systematic understanding of mechanochemistry mechanism is urgently needed. Thiessen *et al.* firstly proposed magma-plasma theory to explain mechanochemistry.[42] In his theory, it is thought that a highly excited plasma-like state, lasting about 10^{-7} s, is formed at the point where two particles are crushed with high energy, which causes instantaneous chemical reaction at the point forming active products, along with unstable products. Many theoretical models have been studied after, but these theories are based on indirect measurements. A time-resolved *in situ* measurement

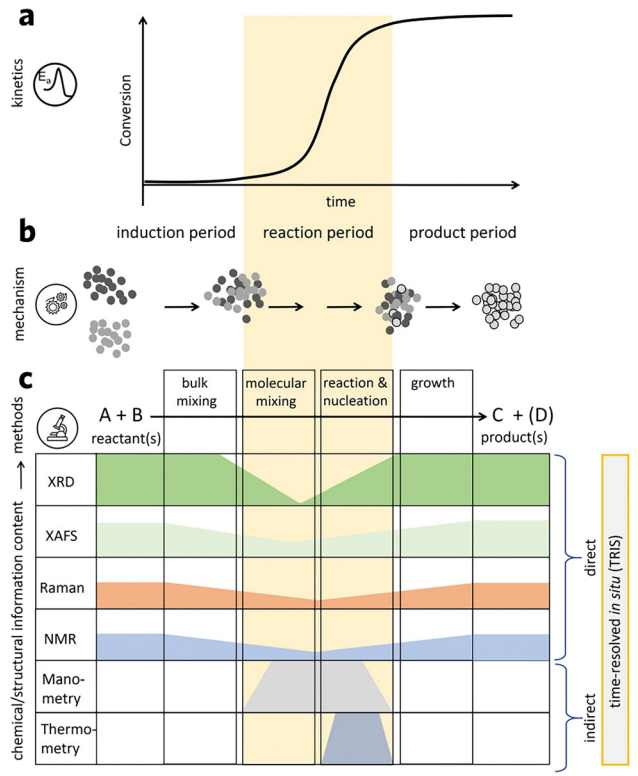

Fig. 4 (a) Possible kinetic profile for mechanochemical synthesis. (b) Macroscopic mechanism description. (c) Existing TRIS methods to characterize mechanochemical transformations. Reproduced with permission from ref. 44.

could provide better insight by looking at what is happening during mechanochemical synthesis. This is extremely useful for organic and metal–organic systems as chemical transitions could happen within a few minutes.[43] Michalchuk *et al.* summarized a 3-step model for mechanochemistry-based time-resolved *in situ* (TRIS) monitoring result (Fig. 4): i) solid state reagents are mixed at both the macroscale and microscale with the help of a medium, such as moving balls; ii) as the milling continues, the physiochemical reaction will happen when the mixing moves to the atomic or molecular level; iii) products start to form from the nucleus to nanocrystalline or microcrystalline phase.[44]

The *in situ* study of mechanochemical synthesis has been conducted to shed light on this process.[45] Early researches mainly focused on monitoring the pressure and temperature during the process, which only offered indirect and limited information. One of the early time-resolved *in situ* measurements on MOFs was performed in 2012 using TRIS powder X-ray diffraction.[46] Subsequently, a follow-up study was performed by the *in situ* monitoring of the milling reaction through both powder XRD and Raman spectroscopy.[47]

Impact of milling parameters

Different miller types, such as shaker mills and planetary mills, have different capacities, speeds, and motion types. The most widely used miller type is the planetary miller owing to its good reproducibility and reliability, and it is commonly used in sample processing, colloidal grinding, and material development.[48] Nevertheless, the impact of miller types on the final products is not as significant compared to other factors.

The size of the miller determines the free space for reaction. If there are not enough free gaps for reactants, the collision will become less effective and hence 50% of free space is recommended to be left as a rule of thumb.[14] Milling time and speed are both critical for mechanochemical synthesis. A proper milling time can increase the yield, form a homogeneous phase, and reduce the particle size. However, if the milling time is too long or too short, incomplete reaction, formation of undesired phase, deformation, and decomposition can happen.[49,50] Milling speed impacts the synthesis in terms of mixing, energy, and heat. Higher milling speed will result in better mixing and conversion but will also generate more energy and heat due to more intensive collision. Extra heat and energy can result in undesired reaction and decomposition,[51] and excessive temperature can directly affect the solid solubility level and phase formation.[52–54]

Milling balls can directly impact the final products' surface morphology, such as surface area and interfacial connection. Larger or higher density balls can result in higher energy and surface activity during collision, which is good for forming a thermodynamically-stable product. On the other hand, smaller or lighter balls can do better in mixing and form amorphous and metastable material phases because they have higher mobility and a long motion trajectory during milling.[14,55] The optimum number of small balls and large balls used will differ in different materials as too many large balls might not mix the reagents well, while too many small balls might not generate enough energy for reactions. Apart from the milling ball itself, the balls to powder weight ratio also plays an important role in the synthesis. At higher ratio, more energy, and heat are produced due to more intensive collision between balls. Therefore, faster energy transfer and mechanical activation could be expected, which might cause decomposition and undesired reaction.

The effect of milling parameters is strongly related to the milled material's mechanical properties, and the relationship between its functionality and mechanical properties therefore require careful consideration.

Mechanochemical synthesis of MOFs and MOF composites

Mechanochemical synthesis of MOFs

Despite the rich history of mechanochemical synthesis, the mechanochemical synthesis of MOFs only started in 2006.[56] Pichon *et al.* ground copper(II) acetate monohydrate and isonicotinic acid (INA) in a 20 mL steel vessel containing a steel ball bearing at an oscillation rate of 25 Hz and maintained it for

10 min to obtain the first mechanochemically synthesized MOF, $[Cu(INA)_2]\cdot 2H_2O$. The only by-product is water, and X-ray diffraction (XRD) characterization of the synthesized material showed good agreement with single-crystal MOF diffraction data along with the absence of unreacted reactants. Since then, more and more MOFs have been reported *via* mechanochemical synthesis.[57–65]

It should be noted that mechanochemical synthesis is not limited to single metal and single linker MOFs as mixed metal and mixed linker MOFs could also be synthesized.[66,67] Thorne *et al.* successfully synthesized mixed metal and mixed linker ZIF-62 ($[Zn(Im)_{2-x}(bIm)_x]$, where Im = imidazole, bIm = benzimidazole) *via* mechanochemical ball milling.[67] By mixing metal sources such as ZnO and organic ligands, namely, imidazole and benzimidazole, with 20 μL DMF in a ball milling jar for mechanical milling, ZIF-62 could be successfully synthesized. The conversion of ZnO to ZIF-62 can be accelerated using 1% zinc acetate dihydrate $[zn(OAc)_2\cdot 2H_2O]$, which acts as both a zinc source and catalyst for the reaction.[68,69] To form mixed metal ZIF-62, $zn(OAc)_2\cdot 2H_2O$ can simply be replaced with $co(OAc)_2\cdot 2H_2O$ without changing other parameters, and mixed metal Zn–Co ZIF-62 could be formed with up to 20% Co substitution. The XRD patterns also suggest that no observable impurities are present, such as ZnO. Unlike the solvothermal synthesis of ZIF-62, where the ligand ratio is hard to control, mechanochemical synthesis allows for its relatively precise control from $[Zn(Im)_{1.95}(bIm)_{0.05}]$ to $[Zn(Im)_{1.75}(bIm)_{0.25}]$. Meanwhile, it also works when it comes to ligand derivatives. For example, we could still precisely control the ligand ratio when we change benzimidazole to its derivative, 5-chlorobenzimidazole (ZIF-76).

The dimensionality of MOFs plays an important role in its application.[70,71] Other than the most common 3-D MOFs, 1-D and 2-D MOFs have also been successfully fabricated mechanochemically.[72,73] An open question in this line of research is that if a metal organic framework has different dimensional phases, could we mechanochemically tune its dimensionality?

Theoretically, mechanochemical tuning is feasible because many external reaction factors are present during the synthesis, such as high temperature and pressure created by ball crushing, as well as assisted solvent addition for better reactivity.[74,75] By varying these external factors, we could possibly change the MOFs' structures (dimensionality). Our group has successfully changed the mechanochemical synthesis product from 3D ZIF-7-I ($Zn(bim)_2$) to 2D ZIF-7-III by adding water (structural template) during milling caused by the hydrolysis of Zn–N bonds.[76] A similar situation was also observed by Haneul and Junhyung—grinding $FeCl_3\cdot 6H_2O$ and sodium fumarate with different solvent mediums can result in both 1D and 3D Fe-MIL-88A ($Fe_3O(C_4H_2O_4)_3$).[77] In the future study of mechanochemical tuning, scientists could also try to vary the reagent amounts. These methods have already been applied to shift the dimensionality of perovskites.[78]

Successfully synthesized MOFs suggest that mechanochemical synthesis can enable a fast, solvent-saving and high purity synthesis of MOF products. Meanwhile, it demonstrates the capability of mechanochemical process in providing all necessary bonding breaking and forming processes with sufficient mechanical energy. Therefore, mechanochemical compositing of the functional material with MOFs is theoretically feasible.

Mechanochemical amorphization of metal organic frameworks

With regards to the MOF, another concern for the mechanochemical treatment is the preservation of MOFs' crystallinity. Mechanochemical treatment, similar to thermal treatment, can lead to the collapse of the framework structure and eventual amorphization,[79] and this phase transition is reversible for some MOFs upon vapor treatment.[80] Densification is also expected with the increase in the milling time due to the transformation from the crystal to the amorphous form and loss of free volume in the framework.[81] If amorphized MOFs have glass forming ability, such as ZIF-62, it will become amorphous after extended milling but it still shows glassy behavior. Successfully formed ZIF-62 mechano-synthesized glass has a glass transition temperature (T_g) ranging from 318 and 411 °C, and this value is significantly different from solvothermally synthesized ZIF-62 glass due to the difference in particle size and possible presence of a large number of defective sites.[82] Mechanochemistry could synthesize some MOFs configuration that could not be fabricated *via* the traditional solvothermal method due to an excessive amount of energy generated during the mechanical process.

Interfacial interaction during the mechanochemical process

During grinding or milling, mechanical energy is created and used for mechanochemical reaction. Apart from effects such as heating and size reduction in particles, new interfaces are also fabricated from the continuous mechanochemical process. However, there are arguments about the exact mechanism driving the formation of the interface between two components. Conventionally, in an interfacial study of alloy metal, Yavari *et al.* proposed that it is the external capillary pressure that forces two components to form an interface.[83] On the other hand, Gente *et al.* suggests that the chemical enthalpy difference between two components at the interface is the driving force for the formation.[84] These two models approach interface formation from different aspects, namely, physical and chemical aspects. From the physical aspect, shearing, grinding, and milling can promote the formation of the atomic-diffusion layer and hence leads to the stable anchoring of the two components.[2] Meanwhile, from the chemical aspect, heat and energy can promote the reaction between the components and chemical connections, such as van der Waals bonds and covalent bonds, which can be formed between two components. Both physical and

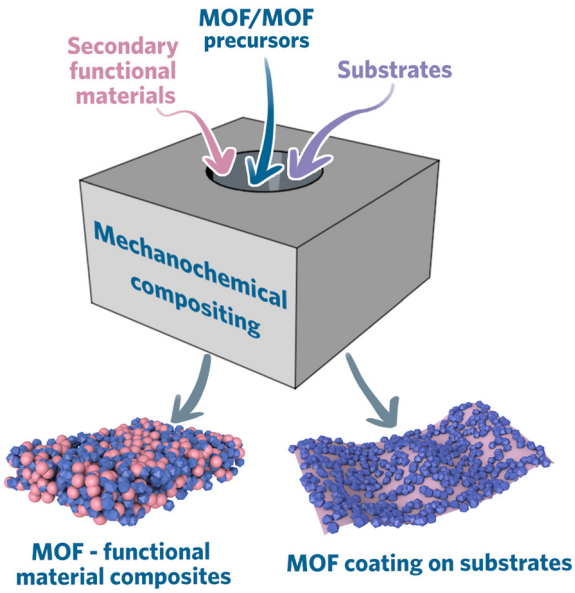

Fig. 5 Schematic summary of mechanochemical compositing routes.

chemical interactions can also exist together, providing an even stronger effect to form composites through the mechanochemical process.

The resultant interfacial bonding and effect can be confirmed *via* various analytical and spectroscopic techniques, such as Fourier-transform infrared spectroscopy (FTIR), terahertz spectroscopy (THZ-IR), X-ray photoelectron spectroscopy (XPS), X-ray absorption, and total scattering analysis. For example, the Sr–O bond seen in FTIR analysis confirmed the formation of the interface between $SrCO_3$–Fe_2O_3 through ball milling.[85]

Mechanochemically synthesized MOF composite

This section will review the materials that have already been composited with MOF *via* mechanochemical synthesis. Generally, there are three ways to mechanochemically synthesize MOF composites: i) direct synthesis from MOF precursors with functional materials; ii) preparation of MOFs and functional materials separately and composite them together mechanochemically; iii) deposition of MOFs on the substrate (coating) (Fig. 5).

Constructing MOF composite directly from MOF precursors

This route requires functional materials to be mechanochemically treated in the presence MOF precursors. Composites are formed during the mechanochemical synthesis of MOFs along with the incorporated functional materials, similar to "building a bottle-around-a-ship" configuration. A benefit of this method is that better protection/encapsulation effect can be expected, with higher flexibility in hosting different sized guest components. This is particularly useful for compositing MOF with fragile guest materials such as enzymes. Enzymes are natural catalysts that have been used in many applications, including food and pharmaceutical industries. Great efforts have been devoted to enhancing their stability, and compositing with MOF is a viable approach. MOFs can offer rigid frameworks to protect biomolecules while enabling the diffusion of reaction substrates and products. Currently, enzyme/MOF composites are mostly synthesized using zeolite imidazole framework (ZIFs) due to its mild and biocompatible synthesis conditions.[86–89] Meanwhile, ZIFs have shown enhanced acidic stability when compositing with enzymes because zinc ions could bond with low pK_a biofunctional groups, such as carboxylate and phosphate groups.[90] These symbiotic effects enable the enzyme to protect ZIFs from acidic operation condition and be protected by the ZIFs matrix from harsh environment. The mechanochemical process offers access to additional framework materials, whose synthetic conditions are normally too harsh for the *in situ* encapsulation of enzymes through the solvothermal process.

In one of the early reports, Wei *et al.* performed a systematic study of four enzymes, namely, β-glucosidase (BGL), invertase, β-galactosidase, and catalase, which retained their functionality after encapsulation by three different MOFs (*i.e.*, ZIF-8, UiO-66 ($Zr_6O_4(OH)_4(BDC)_6$), and ZIF-76) through mechanochemical ball milling synthesis (Fig. 6). They found that the enzymes encapsulated in MOF composites have improved stability against proteases, which is a digestive enzyme that can break down proteins. The enzyme@MOF composites were fabricated by placing all reagents, including MOF precursors and enzymes, in the zirconium-based jar and running the ball mill at a frequency of 8 Hz for 5 min in a Retsch MM400 Mixer Mill machine.[24] They also discovered that the addition of ethanol during compositing could improve the catalyst performance. This could be simply done in mechanochemical synthesis due to the relative ease of controlling the reaction, in comparison to conventional composite synthesis methods such as infiltration method and template synthesis.

This route could also be used in synthesizing MOF composites for biomedical applications, such as MOF–organic drug composites. Traditional solution–infiltration method[91,92] is time-consuming (a few days) and has low drug loading in the composite given that the targeted guest components can be larger than the MOF pore aperture.[93] Metal alloy and ceramic composites have been widely

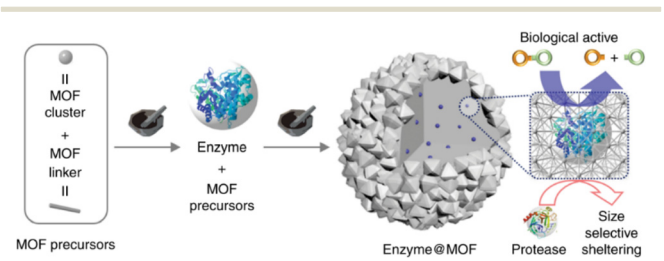

Fig. 6 Two-step mechanochemical approach for embedding glycosidases into MOF. Reproduced with permission from ref. 24.

fabricated *via* mechanochemistry since the last century owing to fast and facile production,[94] but it has not drawn much attention in MOF composite area. One of the works in drug/MOF composites is performed by Jan and co-workers. They explored this method for the synthesis of a composite, namely, ibuprofen/HKUST-1 (IBU/$Cu_3(BTC)_2$).[95] By pre-assembling $[Cu_2(IBU)_4]$·2DMF cluster as MOF precursors, followed by milling with H_3BTC ($C_6H_3(CO_2H)_3$), the composite is successfully synthesized with a 58.5% drug loading, which is higher than the traditional solution-based method. A controlled and complete drug release is realized in a 14 day period.

Apart from microscopic molecules, MOF precursors-based mechanochemical synthesis is also suitable for macroscopic molecules/macrocyclic molecules. Liang *et al.* produced decamethylcucurbit[5]uril/$Fe_3O(H_2O)_2OH(BTC)_2$ (MC5/MIL-100) composite through mechanochemical ball milling. By grinding MC5·2NH_4Cl·4H_2O, $Fe(NO_3)_3$·9H_2O, and H_3BTC crystallites, H_3BTC/Fe-MC5 gel could be synthesized, followed by heating at 160 °C for 5 h to form Fe-MC5/MIL-100 (Fe). During heating, H_3BTC became amorphous due to the dissolution and reaction with iron centers. Hot water is then used to wash out the impurities, and the final product is MC5/MIL-100 (Fe) composites.[96]

The MOF composites discussed so far employ MOFs with high porosity and surface area as the hosted matrix for a functional material. What if the case was reversed, where a mesoporous material acted as a platform for MOF growth within its cavities? The natural question that follows is whether this can be done using mechanochemical milling? Szczęśniak *et al.* approached this question by growing and filling CuBTC MOF in the mesopores of ordered mesoporous carbon (OMC) during mechanochemical processing with the aid of graphene oxide (GO) to facilitate MOF formation in the voids of the mesoporous network.[97] To form OMC/MOF or OMC/GO/MOF composite, additional OMC or OMC/GO is added into the milling vessel during the mechanochemical synthesis of CuBTC MOF (Fig. 7). The morphological information is rather complex, and the MOF structure is only seen in TEM, which is different from pure MOF. Nevertheless, powder XRD confirmed the successful synthesis of three-component composites. In the OMC/MOF composite, when OMC concentration is low (less than 3%), higher pore volume is seen due to the synergistic effect from additional pores.

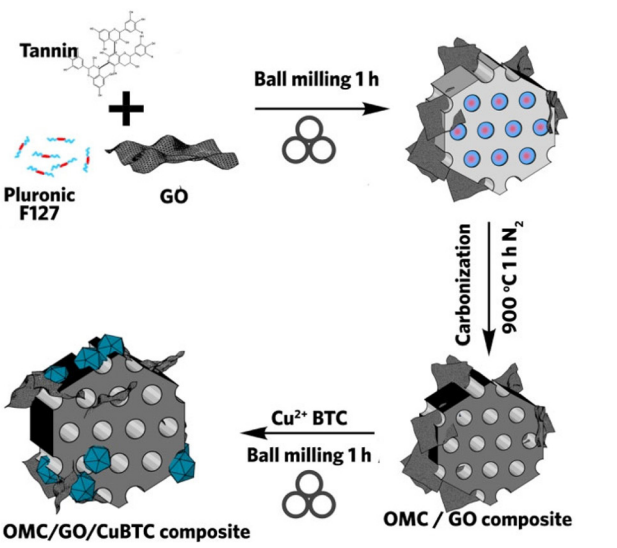

Fig. 7 Schematic procedure of mechanochemically synthesized OMC/GO/CuBTC composite. Reproduced with permission from ref. 97.

Constructing MOF composite *via* the milling of pre-formed MOFs and functional materials

Composites synthesized *via* this route are simply done by mechanically compositing functional materials with pre-formed MOFs. This is the most straightforward route for compositing, similar to the formation of conventional alloys *via* the mechanochemical process. Compositing is mainly achieved by mechanical force, such as stress and compression. In some cases, the external energy may allow the pre-formed MOF to re-organize through covalent bonding breakage and reformation, which will facilitate the hosting of/bonding with the secondary components. An important consideration through this technique is the mechanical robustness of the materials, as the mechanical treatment may lead to deformation, decomposition, or amorphization of the raw materials.

Metal nanoparticles (MNP) for heterogeneous catalysts is a topic of rising interest because we could modify its functionality by simply varying the size, shape, and morphology.[98,99] However, problems such as aggregation could significantly impact its functionality. One of the solutions is the integration of MNPs into the MOF matrix mechanochemically by milling MNPs with MOFs. Ishida *et al.* first deposit Au cluster into five different MOFs (CPL-1 ($[Cu_2(pzdc)_2(pyz)]_n$, pzdc = pyrazine-2,3-dicarboxylate, pyz = pyrazine), CPL-2 ($[Cu_2(pzdc)_2(bpy)]_n$, bpy = 4,4′-bipyridine), MIL-53(Al) ($[Al(OH)(bdc)]_n$), MOF-5, and HKUST-1 ($[Cu_3(btc)_2(H_2O)_3]$)) through mechanochemical treatment.[100] In the following year, similar work was also performed by compositing Au cluster into ZIF-8 by simply grinding dimethyl Au^{III} acetylacetonate with ZIF-8.[101]

Apart from MNP, this type of compositing method can also be applied to small molecules. For example, model drugs including 5-fluorouracil (5FU), caffeine, *para*-aminobenzoic acid (PABA), and benzocaine have been loaded into [Zn_4O(3,5-dimethyl-4-carboxypyrazolato)$_3$] ($[Zn_4O(dmcapz)_3]$) 3D MOF *via* simple mechanochemical ball milling.[102] The composites' showed high loading capacity, ease of control, and excellent stability. It is expected that the highly dynamic treatment conditions facilitated the diffusion of the guest molecules into the pores. Otherwise, the steric hindrance can lead to very low loading capacity through the conventional solvent-based encapsulation process.[95,102]

Perovskites (PVK) have been under the research spotlight due to its unique properties in various optoelectronic and

photonic device applications.[103] However, issues such as stability significantly hinder its application.[104] In the last 10 years, only a few perovskite–MOF composites have been successfully synthesized through the mechanochemical method. Among these, halide perovskite is the most popular one owing to its unique properties in photovoltaic devices.[105] The high tunability of this perovskite material opens great opportunity for further exploration. This includes the variation of the monovalent cation at the center (Cs, MA (methylammonium, CH_3NH_3) or FA (formamidinium, $CH(NH_2)_2$)), the divalent cation (Pb or Sn), and halide X (X = Cl, Br, I, or a combination of them). Bhattacharyya *et al.* synthesized lead halide perovskite ($CsPbX_3$, X = Cl, Br or I)/AMOF-1 ($\{[(NH_2Me_2)_2][Zn_3(L)_2]\cdot 9H_2O\}$ (L = 5,5′-(1,4-phenylenebis(methylene))bis(oxy)diisophthalate) by absorbing Pb(II) into the AMOF-1 and grinding it with CsX to allow on-site $CsPbX_3$ nucleation, generating spatially confined perovskite quantum dot–MOF composites.[21] Many previous researchers have already demonstrated the benefits associated with the size control of perovskite QDs,[106–109] including tuning of the optical band gap while enhancing their stability. Their compositing with MOFs enables a viable technique to reliably tune these properties. A similar study has also been performed on organic-based lead halides ($MAPbBr_3$, MA = methylammonium), as shown in Fig. 8a.[110] Instead of coating cations on the MOFs, Darsi and co-workers used MA-loaded MOF directly. In this case, part of the MOFs is functional groups that react with $PbBr_2$ mechanochemically to form the $MAPbBr_3$@MA-$M(HCOO)_3$ composite. Apart from the metal halide perovskite, another oxygen perovskite could be composited with MOFs *via* a similar mechanochemical compositing method (Fig. 8b).[111]

Aside from these functional materials, MOF itself as a type of hybrid material has also been composited into another MOF to form MOF–MOF composites through multi-step approaches.[112–115] However, the mechanochemical synthesis of MOF–MOF crystal composite has not been reported because compatibility is always a problem with compositing. Recently, we developed a new type of MOF composite comprised of a crystal MOF and a disordered glassy MOF, called a MOF crystal-glass composite (MOF CGC).[116] The fabrication was achieved through milling MOF crystals (MIL-53 or UiO-66) and MOF glass (ZIF-62 glass) for homogenization, followed by thermal treatment. Though the formation of the composite was mainly attributed to the high temperature annealing, increasing evidence suggests the formation of interfacial bonds during the initial milling process, which deserves further investigation.

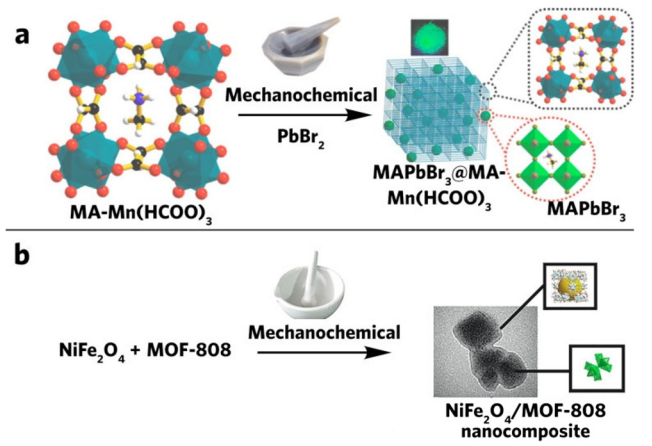

Fig. 8 (a) Synthesis of MAPbBr3@MA-Mn(HCOO)$_3$ *via* solvent-free mechanochemical grinding. Reproduced with permission from ref. 110, (b) mechanochemical synthesis of the $NiFe_2O_4$/MOF-808 composite. Reproduced with permission from ref. 111.

Constructing MOF composite *via* coating MOFs onto substrates (MOF me coating)

The formation of a thin film is usually needed for transferring MOF materials into devices, such as separation membrane, sensor, catalysis, and electrodes. However, the technique that allows the direct bonding of MOF onto non-functionalized substrates is still relatively limited. Given the nature of the mechanochemical process, this enables the direct compositing or coating of pre-formed MOF powders onto substrates for device assembly. The versatile technique circumvents the incompatibility issue between certain MOFs and substrates.

Our group first introduced the formation of MOF glass coating on non-functionalized carbon cloth substrates.[117] The process involves the ball milling of pre-synthesized glass-forming MOF powders with a piece of carbon cloth, generating the stable MOF coating. Given that the substrate is non-functionalized, the direct coating allows efficient electron transfer between the MOF's reactive sites and the conductive substrate. Therefore, the fabricated composite can serve as efficient electrocatalytic electrodes for the oxygen evolution reaction. Glassy composites significantly improved the oxygen evolution reaction,[68] especially Co–Fe bimetallic ZIF-62 glass due to the presence of coordinatively bonded Fe.[118,119] It is worth mentioning that the process is rather facile and rapid: the coating can be realized with merely 5 min of treatment.

In a subsequent study, we further explored the versatility of such a technique by coating different types of MOFs, including ZIF-4 ($Zn(Im)_2$), ZIF-8, and ZIF-67($Co(mIm)_2$), onto various substrates such as carbon cloth, nickel foam, polymeric thin film, titanium foil, and glass slide (Fig. 9).[2] Local heat and mechanical stress created by the mechanochemical process facilitated the interfacial connection and strongly anchored MOFs on the non-functional materials. Ease of operation and scalable production lead to the hope of processable and controllable MOF devices.

MOFs have also been widely composited with polymers to form functional thin films for use in many different applications. Although extensive research has been performed to understand the mechanochemistry of MOF and

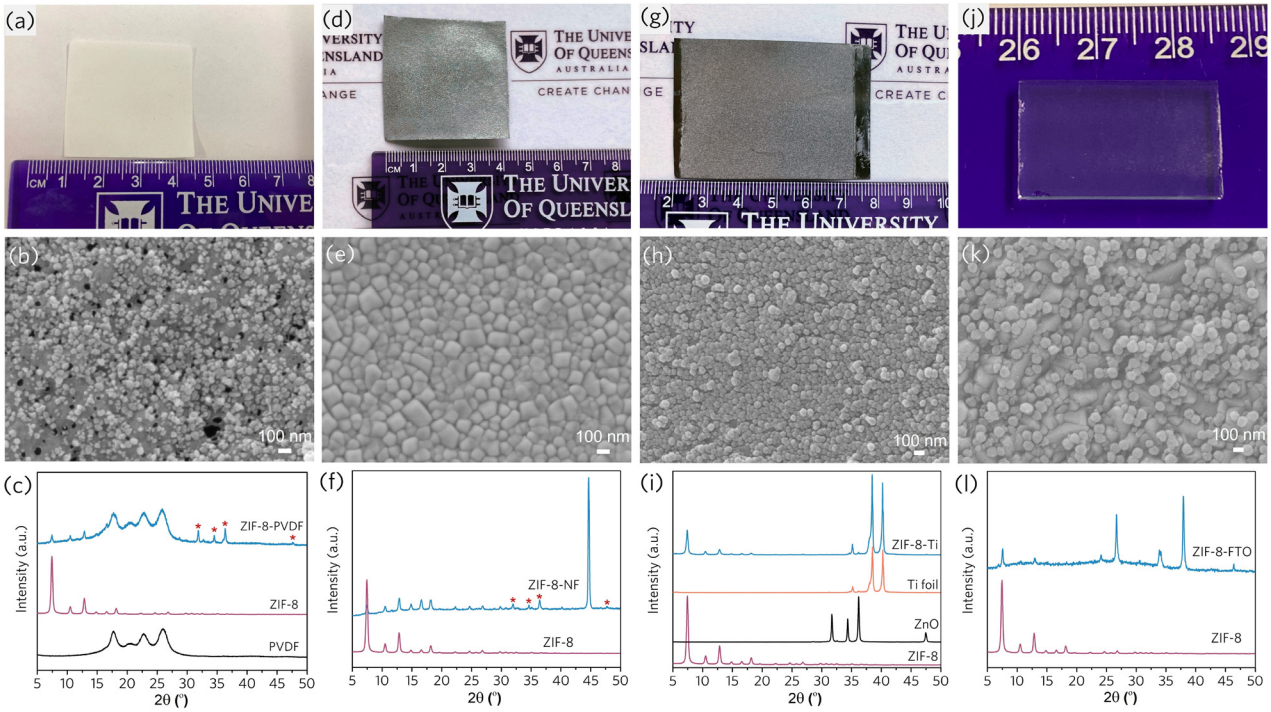

Fig. 9 Mechanochemical coating of ZIF-8 on various substrates: (a–c) one-pot coating on PVDF from ZIF-8 precursors, (d–f) one-pot coating on nickel foam (NF) from ZIF-8 precursors, (g–i) one-pot coating on Ti foils from ZIF-8 precursors, (j–l) ZIF-8 coating on FTO glass. Reproduced with permission from ref. 2.

polymer formation, only a few studies have been conducted on MOF–polymer composite formation *via* mechanochemistry.[57,120–123] Our group has demonstrated the capability of MOF composite formation onto PVDF polymeric membrane, showing good interfacial interaction of the synthesized MOFs onto the non-functionalized polymeric substrate.[2] This approach opens a new possible application of the polymer–MOF composite with fast and facile one-pot synthesis and no pre-functionalization requirement.

Applications of mechanochemically synthesized MOF composites

Apart from the short reaction time, little solvent usage, and ease of fabrication compared to conventional solution-based methods, MOF composite fabricated *via* mechanochemical compositing can also have smaller particle size, larger surface area, better porosity/diffusion, and better mechanical robustness due to the high energy mechanical process.[124] These advantages enable mechanochemically synthesized composites to offer new opportunities in many applications.[100] The applications are summarized in Table 1.

Catalysis

A catalyst used in the fine chemicals industry must have a high product selectivity. Among various nanoparticle composite catalysts, MOF-nanoparticle composites have shown a great potential in particular due to the presence of active sites in the MOFs, and the encapsulation of catalysts in MOFs has already shown promising results in various disciplines.[33,125–128] Furthermore, the nanoparticle catalysts can be controllably integrated with MOFs *via* mechanochemical methods.[129]

Haruta and co-workers deposited gold clusters into MOFs (CPL-1, CPL-2, MIL-53(Al), MOF-5, and HKUST-1) through hand grinding (Fig. 10a) and found that the composites showed much higher catalytic activity (91% conversion rate) in the aerobic oxidation of alcohols than the parent materials.[100] They also observed that the composites tend to have smaller mean diameter size with more uniform particle distribution compared to the traditional chemical vapor deposition method. The composites' particle size is associated with the type of MOF used in grinding, suggesting that different structures, pore sizes, and surface nature of MOFs could alter the dimensions of the composite. For example, Au/CPL-2 has a cluster size of 2.2 ± 0.3 nm and Au/MIL-53 has a cluster size of 1.5 ± 0.7 nm, but they are all smaller than Au nanoparticles yielded from chemical vapor deposition.[100] Small size benefits are found in the following research.[130] It was found that the favorable small size of Au@MIL-53 can promote the catalytic synthesis of amines, such as one-pot synthesis of secondary amines from primary amines by sequential oxidation/hydrogenation, and the hydrogenation of imine to amine. In the following year, Jiang *et al.* successfully deposited Au in ZIF-8 through hand milling and produced the Au/ZIF-8 nanocomposite with different loading, which showed great potential as a CO oxidation

Table 1 Summary of applications

Application	MOF	Functional material	Composting type[a]	Performance	Ref.
Catalysis	CPL-1, CPL-2, MIL-53(Al), MOF-5, and HKUST-1	Au clusters	Type 2	Mechanochemically synthesized catalysts Au/MOF-5 composite can reach 91% and 79% yield in the oxidation of benzyl alcohol and 1-phenylethanol, respectively	100
	MIL-53(Al)	Au clusters	Type 2	The mean diameter of Au particles in the Au/MIL-53 composite could be minimized to 1.6 ± 1.0 nm and the composite can reach 91% yield in the synthesis of dibenzylamine	130
	ZIF-8	Au nanoparticles	Type 2	CO oxidation behavior is enhanced with increased amount of Au inside the composite with 50% conversion temperature, which is decreased to 170 °C at 5% Au in ZIF-8	101
	UIO-66-NH_2	β-Glucosidase (BGL)	Type 1	After exposure to protease in acidic condition (pH = 6), the free BGL and BGL/ZIF-8 composite only retained 16% and 40% activity, respectively, while BGL/UiO-66-NH_2 composite could retain about 90% of its activity. The outstanding enzyme activity retention of BGL/UiO-66-NH_2 was due to the stability of UiO-66-NH_2 under acidic condition, which protected BGL from protease. On the other hand, ZIF-8 was unstable in acidic condition, which exposed the BGL to hydrolysis by protease	24
	ZIF-8 (Zn, Co, ZN/Co)	1-Methyl-3-propylimidazolum bromide (ionic liquid, IL)	Type 1	IL/ZIF-8 (Zn/Co) composite reaches 99% yield in cycloaddition of CO_2. Reaction conditions: epichlorohydrin (10.8 mmol), IL/ZIF-8 (Zn/Co) (100 mg), 24 h, 100 °C, and 1 atm of CO_2	133
	MOF-808	$NiFe_2O_4$	Type 2	$NiFe_2O_4$/MOF-808 composite has great capability in visible-light photocatalytic meropenem degradation and Cr(VI) reduction with 100% efficiency at pH = 2 within 60 min for Cr(VI) reduction and 100% in 60 min for meropenem degradation	111
Adsorption	CuBTC	Mesoporous carbon (OMC) and graphene oxide (GO)	Type 1	1–3% wt% OMC added into CuBTC could result in larger surface area (from 1830 $m^2\ g^{-1}$ to 1930 $m^2\ g^{-1}$) for CO_2 adsorption due to optimal combination between MOF and OMC in the composite	97
	HKUST-1	Imidazole	Type 1	$IM_{1\%}$/HKUST-1 composite has excellent SF_6 adsorption capacity (5.98 mmol g^{-1} at 1 bar and 25 °C) with up to 93 SF_6/N_2 selectivity at 1 bar and water stability	143
	MIL-100(Fe)	Decamethylcucurbit[5]uril (MC5)	Type 1	MC5/MIL-100(Fe) showed better Pb(II) removal efficiency (99.7%) compared to the parent materials (53% and 8%, respectively). Even in the presence of 100 ppm competing ions, such as Na^+, K^+, Mg^{2+}, and Ca^{2+}, over 73% Pb(II) could still be removed	96
	TpPa-1	Magnetic carbon nanotubes (MCNTs)	Type 1	MCNTs/TpPa-1 showed outstanding adsorption capacity of three types of MCs (MC-RR, MC-YR, and MC-LR) with maximum adsorption capacity (Q_{max}) of about 120.8, 209.6, and 244.7 μg g^{-1}, respectively	144
Energy storage	ZIF-8	Si	Type 1	The Si/ZIF-8 composite has superior electrochemical properties with up to 1050 mA h g^{-1} lithium storage as well as excellent cycle stability (>99% capacity retention after 500 cycles) and rate performance	151
	ZIF-8	Carbon/S_8	Type-1/type-2	Positive electrode ZIF-8/C/S_8 composite showed initial discharges of 772 mA h g^{-1}, showing 54% improvement compared with pristine ZIF-8/S8. Meanwhile, the Li_2S_6 absorption tests confirms the ZIF-8/C/S_8 better polysulfides absorption with 87% discoloration	152
	CoBTC	Graphene sheet (GNS)	Type-2	The GNS/CoBTC composite shows high specific capacitance of 608.2 F g^{-1} at current density of 0.25 A g^{-1} in 1 M KOH electrolyte with about 95% capacitance retention after 2000 cycles	124
	NENU-3	Imidazole	Type-1	The IM/NENU-3 composite shows increase in the proton conductivity and varies from 5.79×10^{-4} S cm^{-1} at 298 K to 7.06×10^{-3} S cm^{-1} at 338 K, with tremendous improvement compared to the original	1

Table 1 *(continued)*

Application	MOF	Functional material	Composting type[a]	Performance	Ref.
				NENU-3 (only 4.97×10^{-6} S cm^{-1} at 338 K). Meanwhile, the composite conductivity could be further tuned by changing the relative humidity (RH)	
Energy generation	ZIF-8	BODIPY dye PM605	Type-1	PM605@ZIF-8 materials show enhanced emissive properties with an unprecedented ~10-fold better BODIPY photostability. 0.5% PM605 in the composite shows the best fluorescence intensity	159
	AMOF-1	Halide perovskite quantum dots	Type-2	The composites exhibited stable, narrow, and high luminescence from peaks at 412 nm to 695 nm with better size distribution	21
	MA-M$(HCOO)_3$ (M = Mn or Co)	$MAPbBr_3$	Type-2	Mechanochemically-fabricated MA-M$(HCOO)_3$/$MAPbBr_3$ composites exhibit noticeable improvement in the luminescence with outstanding stability in various solvents, such as water and ethanol, for over 15 days	110

[a] Type 1-MOF precursor + functional material, type 2-preformed MOF + functional material.

catalyst. By applying this material to catalyze the CO oxidation reaction, improved performance was seen in the composite compared to pure ZIF-8, with the 5% Au/ZIF-8 composite showing the best performance that reached half conversion at about 170 °C.[101] This demonstrated the possibility of loading various noble metals into the MOF network.[101,131]

Wei *et al.* used mechanochemical milling to successfully composite enzymes such as β-glucosidase (BGL), invertase, β-galactosidase, and catalase with ZIF-8, UiO-66, and ZIF-76. The BGL/UiO-66-NH_2 composite showed great performance and stability in the acidic condition due to its acidic resistance and large aperture size of ~6.0 Å, while BGL/ZIF-8 had no apparent activity due to the smaller pore size of ZIF-8 (~3.4 Å).[24] Apart from improving the functionality and stability of the enzyme, enhanced immobilization of the hosted catalyst could also be achieved through the mechanical amorphization of the MOF composite.[132] By amorphorizing calcein or α-cyano-4-hydroxycinnamic acid (α-CHC)-loaded Zr-based MOFs *via* ball milling, slower drug release was observed.

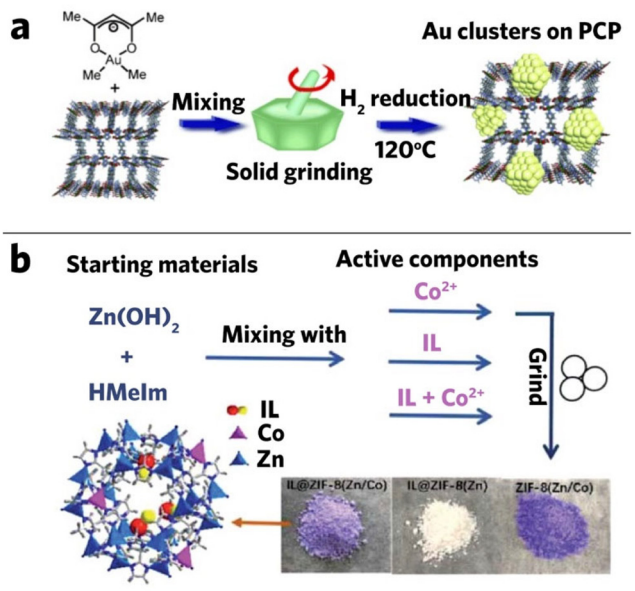

Fig. 10 (a) Mechanochemical deposition of gold clusters on porous coordination polymers. Reproduced with permission from ref. 100, (b) synthetic procedures of L@ZIF-8(Zn/Co). Reproduced with permission from ref. 133.

Imidazolium-based ionic liquids are considered as good catalysts, but their application is hindered by complicated separation procedures. Sun *et al.* successfully combined ionic liquid (1-methyl-3-propylimidazolium bromide, MPImBr) with ZIF-8 and fabricated the IL/ZIF-8 composite. Mixed metal composite could also be formed by simply adding metal salts during mixing (Fig. 10b). The catalytic performance of the composite has shown significant enhancement, reaching 99% yield in the cycloaddition of CO_2 and epoxide.[133]

In the photocatalyst field, Negi and co-workers used ferrite/MOF composite as a photocatalyst by simply grinding $NiFe_2O_4$ together with MOF-808 $[Zr_6O_5(OH)_3(BTC)_2(HCOO)_5(H_2O)_2$, BTC = 1,3,5-benzenetricarboxylate]. The synthesized composite demonstrated great capability in visible-light photocatalytic meropenem degradation and Cr(VI) reduction, having 100% efficiency at pH = 2 within 60 min for Cr(VI) reduction and 100% in 60 min for meropenem degradation. The composites' outstanding photocatalytic performance is the result of increased surface area and active sites.[111]

Adsorption

Due to unique porosity and functional groups, MOF itself has already been employed as a great candidate for adsorption, including gas adsorption,[134] water treatment,[135,136] and specific ion adsorption.[137] The integration of MOFs with other porous materials has demonstrated great potential in increasing their adsorption ability compared with the parent materials.[138,139–142] Compared to traditional methods such as solvothermal method, larger surface area, better porosity,

and structure robustness make mechanochemically-fabricated MOF composites more appealing.

For gas adsorption, Szczęśniak *et al.* mechanochemically composited mesoporous carbon (OMC) and graphene oxide (GO) into CuBTC, and observed improved porosity and CO_2 adsorption capacity in the 1–3% OMC/MOF composites compared with the parent materials, which is suggested to be due to the optimal combination between MOF and OMC in the composite and the additional porosity created by the compositing.[97] Additional porosity and surface area promote CO_2 adsorption capacity. Similarly, Liu *et al.* demonstrate that Im@HKUST-1 could selectively adsorb harmful greenhouse gas SF_6 with outstanding cyclability and water resistance.[143]

In an extraction study, Liang *et al.* mechanochemically composited macroscopic cage-like monolithic decamethylcucurbit[5]uril (MC5) into MIL-100(Fe). The composites have outstanding lead capture ability even at low concentration. Compared to pure MIL-100(Fe) and solid $MC5{\cdot}2NH_4Cl{\cdot}4H_2O$, the composite showed improved Pb(II) removal efficiency (99.7%) compared to the parent materials (53% and 8% respectively). Even in the presence of competing ions, such as Na^+, K^+, Mg^{2+}, and Ca^{2+}, the efficiency was still relatively high. These findings demonstrate the ability of mechanochemical synthesis in producing macroscopic porous composite materials.[96] The same year, Liu *et al.* synthesized another MOF composite by grinding magnetic carbon nanotubes (MCNTs), *p*-toluenesulfonic acid (PTSA), *p*-phenylenediamine (Pa-1), and 1,3,5-triformylphloroglucinol (Tp), which exhibited great adsorption ability in water. The composite has great water dispersibility, large surface area, and high affinity toward microcystins (MCs). The adsorption study of the composite in lake water samples showed outstanding adsorption capacity of three types of MCs (MC-RR, MC-YR, and MC-LR) with maximum adsorption capacity (Q_{max}) of about 120.8, 209.6, and 244.7 μg g^{-1}, respectively. Furthermore, the composite showed better enrichment performance of the MCs compared to MCNTs.[144]

Energy storage

Energy storage is another hot topic for MOF composites. The pores of the MOFs could provide space for transferring cations and electrochemical reaction[145,146] while the hosted material, such as metal oxide or graphene, could provide different functions. For example, metal oxide could supply active redox sites.[26,27,147] Pioneering works have already been done using MOF composite as the supercapacitor,[148] energy storage material,[149] and anode[150] *via* template synthesis.

One of the early mechanochemical attempts was performed by Han and co-workers, who fabricated the Si/ZIF-8 composite *via* mechanochemical synthesis and demonstrated its ability to be used as the anode in a lithium-ion battery. The composite had a lithium storage capacity of up to 1050 mA h g^{-1} with 99% capacity retention after 500 cycles at only about 7% Si loading in the composite. It was suggested that encapsulating with ZIF-8 could mitigate the Si volume change during operation to ensure that it is in close contact with the conductors. Meanwhile, the uniform metal distribution of ZIF-8 could help to improve conductivity in the matrix structure, which is beneficial for Li ion transportation during operation. Even though only a small amount of Si is applied, the fast synthesis and promising performance enable it to be an ideal substitute for high energy anode and open the gate for mechanochemically-synthesized MOF composites in electrodes.[151] A similar study has also been performed to circumvent Li–S battery problems.[152]

Apart from the lithium battery, a follow up study has employed MOF composites in supercapacitors to further expand its application. Supercapacitors have been a hot topic recently not only due to their application in renewable energy technologies but also its high energy storage density and shorter charging time compared with conventional energy sources, such as batteries.[153] Punde *et al.* synthesized cobalt-based MOF CoBTC/graphene sheet nanocomposite *via* grinding. Compositing MOF with graphene effectively mitigated the restacking problem because CoBTC rods are placed between graphene, which is used as a support. Consequently, extremely high specific capacitance of 608.2 F g^{-1} was found at a current density of 0.25 A g^{-1} in 1 M KOH

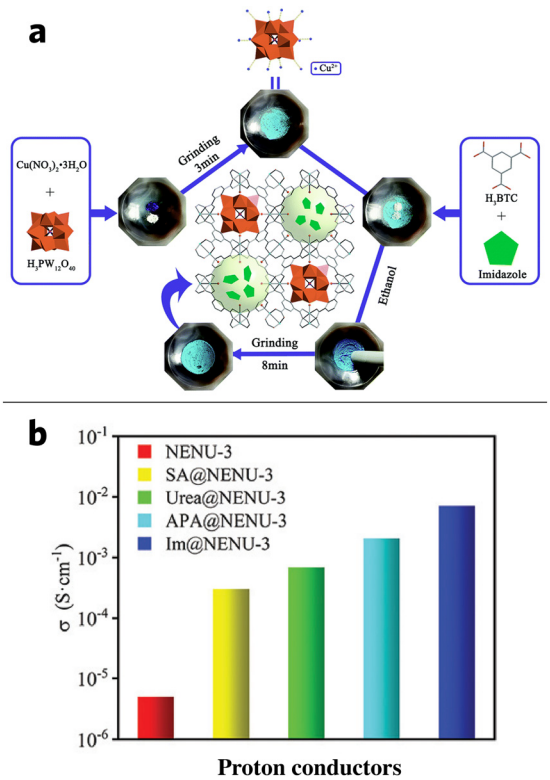

Fig. 11 (a) Schematic procedure of mechanochemically synthesized IM/MOF composite (b) the comparison of proton conductivity of the guest@NENU-3 composite and NENU-3 @338k. Reproduced with permission from ref. 1.

electrolyte, with about 95% capacitance retention after 2000 cycles.[124] In addition, Punde and co-workers also compared mechanochemical MOFs composite with solvothermal MOFs composite; better performance is observed in the former because of its large surface area and better porosity for diffusion.

Wang *et al.* attempted to composite imidazole (IM) into NENU-3 ($[Cu_{12}(BTC)_8(H_2O)_{12}]$ $[H_3PW_{12}O_{40}]\cdot nH_2O$, H_3BTC = 1,3,5-benzentricaboxylate) *via* mechanochemical grinding. As the following scheme in Fig. 11a shows, IM can be grinded into NENU-3 through simple one-pot grinding, which provides a fast and facile way to produce IM/MOF composite that requires only a small amount of ethanol compared to solution immersion[154,155] and chemical vapor deposition methods.[156] The BET surface area of NENU-3 is 538 $m^2\ g^{-1}$, while the BET surface area of IM@NENU-3 reduced by almost half at 274 $m^2\ g^{-1}$, indicating the presence of IM in the pores. An increase in the proton conductivity of 5.79×10^{-4} S cm^{-1} at 298 K and up to 7.06×10^{-3} S cm^{-1} at 338 K (Fig. 11b) was observed in the composite, compared to the original NENU-3 with only 4.97×10^{-6} S cm^{-1} at 338 K. This is equivalent to an increase by almost three orders of magnitude. Meanwhile, the composite conductivity could be further tuned by changing the relative humidity (RH) to 95%.[1]

Energy generation

Energy generation has drawn increasing attention in the past few decade, especially for clean and sustainable energy generation *via* photocatalysis.[157,158] High fluorescence material could also be synthesized *via* ion and liquid-assisted ball milling. By compositing commercial BODIPY dye PM605 into ZIF-8, the PM605@ZIF-8 composite was formed that is highly emissive, photostable, and microporous (Fig. 12). Meanwhile, this strategy could be used to encapsulate other BODIPY systems, such as PM546, HCIBOH, and PM650, yielding high emission and providing a facile method to include fluorophores within MOF.[159] One year later, Bhattacharyya *et al.* synthesized perovskite quantum dots (PQDs)/AMOF-1 composite with high stability and processibility. The composite exhibited stable, narrow, and high luminescence from the peaks at 412 nm to 695 nm (Cl–Br–I).[21] Narrow luminescence results indicate good size contribution due to quantum confinement.[160] Similar work was performed by Rambabu and co-workers on organic–inorganic lead halide ($MAPbBr_3$) perovskite and a stable, narrow, and high luminescence was seen.[110] Previously, $MAPbBr_3$ has already been reported to be stabilized by oleic acid.[161] Comparing with the reported oleic acid-stabilized $MAPbBr_3$, the mechanochemical synthesized composite showed far superior stability and could exist in various solvents for over 15 days.

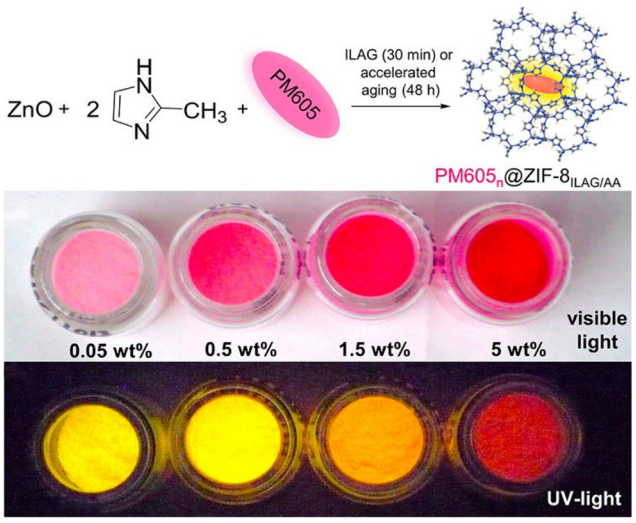

Fig. 12 Schematic procedure of mechanochemically synthesized PM605/ZIF-8 composite. Reproduced with permission from ref. 159.

Conclusions and perspective

The integration of functional materials into the MOF matrix allows for the utilization of the MOFs' high surface area and porosity to protect the functional materials from external environmental factors, resulting in enhanced stability and functionality. Compared to infiltration synthesis and template synthesis, mechanochemical synthesis provides a fast, facile, green, and convenient way to produce the MOF composite, with better structural robustness, porosity, and smaller particle sizes, endowing the composite with great potentials in many application fields. Furthermore, large scale production is also more feasible *via* mechanochemical synthesis.

However, this does not mean ball milling is a perfect all-rounder. Excessive mechanical energy generated during milling could lead to the amorphization of MOFs and decomposition or damage to the functional materials, which strictly limits the selection of the applied materials. Meanwhile, impurities are more likely to occur, especially in hand milling, causing difficulties for future applications. The biggest problem about mechanochemistry is the poor understanding of the mechanism, and hence scientists cannot have full control of the modern mechanochemical synthesis, which necessitates deeper and more systematic understanding of the mechanochemical mechanism. *In situ* spectroscopic analysis of the product/composite during synthesis would be highly desirable, although highly challenging due to high-speed movement.

Future studies on the mechanosynthesis of MOF composites may see the increased use of an emerging class of MOFs known as MOF glass, which can be an effective hosting matrix in addition to MOF crystals due to increased processability and interaction with functional materials during melting. In addition, interfacial defects in the MOF composites can also be regulated and eliminated through heat treatment.

The construction of a mixed-matrix architecture *via* the mechanochemistry for MOF–MOF composites has a unique benefit in that the issue of lattice mismatch with other crystalline MOFs can be avoided. The implementation of glassy MOFs as the shell can further promote interfacial chemical bonding with the core MOF due to the formation of a liquid state upon melting.

Although the product obtained from mechanochemical synthesis is typically in the form of a solid powder, it can be further applied to form a coating on the substrates *in situ*. It is possible to transfer MOF powders as a coating onto a non-prefunctionalized substrate such as porous polymer membranes or carbon cloth using the mechanochemical route.[2] This is due to the generation of surface oxide functional groups and atomic inter-diffusion layer by the high energy mechanochemical treatment for the stable anchoring of MOFs to the substrates. We imagine that with further regulation and optimization of the milling parameters, the mechanochemical synthesis of MOF composites can be coupled with the *in situ* formation of a coating on a substrate. It should be acknowledged that this would be difficult to implement at the current stage due to the poor understanding of the mechanochemistry mechanism surrounding MOF synthesis, but with increasing studies, this could be achievable. This would not only improve the recyclability of the MOF composites but also enable their synthesis and assembly in practical devices in one step, with minimal or no wastage of solvents and products.

Conflicts of interest

The authors declare no conflict of interest.

Acknowledgements

W. W. would like to thank Australian government and the University of Queensland for the Graduation School Scholarship support. J. H. acknowledges the financial support from the Australian Research Council (FT210100589) and the University of Queensland (2021002771). V. C. acknowledges funding by the Australian Government through the Australian Research Council through its Discovery Program (DP180103874).

Notes and references

1 Y. Wang, Y. Lu, Z. Li, X.-W. Sun, W.-Y. Zhang, S. Zhang, J. Wang, T.-Y. Dang, Z. Zhang and S.-X. Liu, One-pot mechanochemical synthesis to encapsulate functional guests into a metal–organic framework for proton conduction, *Chem. Commun.*, 2021, **57**(71), 8933–8936.

2 R. Lin, Y. Yao, M. Y. B. Zulkifli, X. Li, S. Gao, W. Huang, S. Smart, M. Lyu, L. Wang, V. Chen and J. Hou, Binder-free mechanochemical metal–organic framework nanocrystal coatings, *Nanoscale*, 2022, **14**(6), 2221–2229.

3 C. Xu, S. De, A. M. Balu, M. Ojeda and R. Luque, Mechanochemical synthesis of advanced nanomaterials for catalytic applications, *Chem. Commun.*, 2015, **51**(31), 6698–6713.

4 Y. Wang, H. Wang, Y. Jiang, C. Zhang, J. Shao and D. Xu, Fast, solvent-free and highly enantioselective fluorination of β-keto esters catalyzed by chiral copper complexes in a ball mill, *Green Chem.*, 2017, **19**(7), 1674–1677.

5 M. Vadivelu, S. Sugirdha, P. Dheenkumar, Y. Arun, K. Karthikeyan and C. Praveen, Solvent-free implementation of two dissimilar reactions using recyclable CuO nanoparticles under ball-milling conditions: synthesis of new oxindole-triazole pharmacophores, *Green Chem.*, 2017, **19**(15), 3601–3610.

6 H. Xu, H.-W. Liu, K. Chen and G.-W. Wang, One-Pot Multicomponent Mechanosynthesis of Polysubstituted trans-2,3-Dihydropyrroles and Pyrroles from Amines, Alkyne Esters, and Chalcones, *J. Org. Chem.*, 2018, **83**(11), 6035–6049.

7 M. Turberg, K. J. Ardila-Fierro, C. Bolm and J. G. Hernández, Altering Copper-Catalyzed A3 Couplings by Mechanochemistry: One-Pot Synthesis of 1,4-Diamino-2-butynes from Aldehydes, Amines, and Calcium Carbide, *Angew. Chem., Int. Ed.*, 2018, **57**(33), 10718–10722.

8 Q. Cao, R. T. Stark, I. A. Fallis and D. L. Browne, A Ball-Milling-Enabled Reformatsky Reaction, *ChemSusChem*, 2019, **12**(12), 2554–2557.

9 Y. X. Shi, K. Xu, J. K. Clegg, R. Ganguly, H. Hirao, T. Friščić and F. García, The First Synthesis of the Sterically Encumbered Adamantoid Phosphazane P4(NtBu)6: Enabled by Mechanochemistry, *Angew. Chem., Int. Ed.*, 2016, **55**(41), 12736–12740.

10 A. D. McNaught and A. Wilkinson, *Compendium of chemical terminology*, Blackwell Science Oxford, 1997, vol. 1669.

11 L. Takacs, The historical development of mechanochemistry, *Chem. Soc. Rev.*, 2013, **42**(18), 7649–7659.

12 K. Horie, M. Barón, R. B. Fox, J. He, M. Hess, J. Kahovec, T. Kitayama, P. Kubisa, E. Maréchal, W. Mormann, R. F. T. Stepto, D. Tabak, J. Vohlídal, E. S. Wilks and W. J. Work, Definitions of terms relating to reactions of polymers and to functional polymeric materials (IUPAC Recommendations 2003), *Pure Appl. Chem.*, 2004, **76**(4), 889–906.

13 D. A. Giannakoudakis, G. Chatel and J. C. Colmenares, Mechanochemical Forces as a Synthetic Tool for Zero- and One-Dimensional Titanium Oxide-Based Nano-photocatalysts, *Top. Curr. Chem.*, 2019, **378**(1), 2.

14 D. Ozer, Mechanochemistry: A Power Tool for Green Synthesis, in *Advances in Green Synthesis: Avenues and Sustainability, Inamuddin*, ed. R. Boddula, M. I. Ahamed and A. Khan, Springer International Publishing, Cham, 2021, pp. 23–39.

15 M. Pérez-Venegas and E. Juaristi, Mechanochemical and Mechanoenzymatic Synthesis of Pharmacologically Active Compounds: A Green Perspective, *ACS Sustainable Chem. Eng.*, 2020, **8**(24), 8881–8893.

16 B. Szczęśniak, S. Borysiuk, J. Choma and M. Jaroniec, Mechanochemical synthesis of highly porous materials, *Mater. Horiz.*, 2020, **7**(6), 1457–1473.

17 P. Ying, J. Yu and W. Su, Liquid-Assisted Grinding Mechanochemistry in the Synthesis of Pharmaceuticals, *Adv. Synth. Catal.*, 2021, **363**(5), 1246–1271.
18 D. Lyu, W. Xu, J. E. L. Payong, T. Zhang and Y. Wang, Low-dimensional assemblies of metal-organic framework particles and mutually coordinated anisotropy, *Nat. Commun.*, 2022, **13**(1), 3980.
19 G. Chen, L. Tong, S. Huang, S. Huang, F. Zhu and G. Ouyang, Hydrogen-bonded organic framework biomimetic entrapment allowing non-native biocatalytic activity in enzyme, *Nat. Commun.*, 2022, **13**(1), 4816.
20 Z. Li, F. Jiang, M. Yu, S. Li, L. Chen and M. Hong, Achieving gas pressure-dependent luminescence from an AIEgen-based metal-organic framework, *Nat. Commun.*, 2022, **13**(1), 2142.
21 S. Bhattacharyya, D. Rambabu and T. K. Maji, Mechanochemical synthesis of a processable halide perovskite quantum dot–MOF composite by post-synthetic metalation, *J. Mater. Chem. A*, 2019, **7**(37), 21106–21111.
22 S. Zheng, Q. Li, H. Xue, H. Pang and Q. Xu, A highly alkaline-stable metal oxide@metal–organic framework composite for high-performance electrochemical energy storage, *Natl. Sci. Rev.*, 2019, **7**(2), 305–314.
23 M. Bellusci, P. Guglielmi, A. Masi, F. Padella, G. Singh, N. Yaacoub, D. Peddis and D. Secci, Magnetic Metal–Organic Framework Composite by Fast and Facile Mechanochemical Process, *Inorg. Chem.*, 2018, **57**(4), 1806–1814.
24 T.-H. Wei, S.-H. Wu, Y.-D. Huang, W.-S. Lo, B. P. Williams, S.-Y. Chen, H.-C. Yang, Y.-S. Hsu, Z.-Y. Lin, X.-H. Chen, P.-E. Kuo, L.-Y. Chou, C.-K. Tsung and F.-K. Shieh, Rapid mechanochemical encapsulation of biocatalysts into robust metal–organic frameworks, *Nat. Commun.*, 2019, **10**(1), 5002.
25 J. Hou, A. F. Sapnik and T. D. Bennett, Metal–organic framework gels and monoliths, *Chem. Sci.*, 2020, **11**(2), 310–323.
26 X. Lian, Y. Fang, E. Joseph, Q. Wang, J. Li, S. Banerjee, C. Lollar, X. Wang and H.-C. Zhou, Enzyme–MOF (metal–organic framework) composites, *Chem. Soc. Rev.*, 2017, **46**(11), 3386–3401.
27 J. Yu, C. Mu, B. Yan, X. Qin, C. Shen, H. Xue and H. Pang, Nanoparticle/MOF composites: preparations and applications, *Mater. Horiz.*, 2017, **4**(4), 557–569.
28 C. Zlotea, R. Campesi, F. Cuevas, E. Leroy, P. Dibandjo, C. Volkringer, T. Loiseau, G. Férey and M. Latroche, Pd Nanoparticles Embedded into a Metal-Organic Framework: Synthesis, Structural Characteristics, and Hydrogen Sorption Properties, *J. Am. Chem. Soc.*, 2010, **132**(9), 2991–2997.
29 S. Hermes, M.-K. Schröter, R. Schmid, L. Khodeir, M. Muhler, A. Tissler, R. W. Fischer and R. A. Fischer, Metal@MOF: Loading of Highly Porous Coordination Polymers Host Lattices by Metal Organic Chemical Vapor Deposition, *Angew. Chem., Int. Ed.*, 2005, **44**(38), 6237–6241.
30 Y. Xue, S. Zheng, H. Xue and H. Pang, Metal–organic framework composites and their electrochemical applications, *J. Mater. Chem. A*, 2019, **7**(13), 7301–7327.
31 J. Hou, P. D. Sutrisna, T. Wang, S. Gao, Q. Li, C. Zhou, S. Sun, H.-C. Yang, F. Wei and M. T. Ruggiero, Unraveling the Interfacial Structure–Performance Correlation of Flexible Metal–Organic Framework Membranes on Polymeric Substrates, *ACS Appl. Mater. Interfaces*, 2019, **11**(5), 5570–5577.
32 A. Aijaz, A. Karkamkar, Y. J. Choi, N. Tsumori, E. Rönnebro, T. Autrey, H. Shioyama and Q. Xu, Immobilizing Highly Catalytically Active Pt Nanoparticles inside the Pores of Metal–Organic Framework: A Double Solvents Approach, *J. Am. Chem. Soc.*, 2012, **134**(34), 13926–13929.
33 G. Lu, S. Li, Z. Guo, O. K. Farha, B. G. Hauser, X. Qi, Y. Wang, X. Wang, S. Han, X. Liu, J. S. DuChene, H. Zhang, Q. Zhang, X. Chen, J. Ma, S. C. J. Loo, W. D. Wei, Y. Yang, J. T. Hupp and F. Huo, Imparting functionality to a metal–organic framework material by controlled nanoparticle encapsulation, *Nat. Chem.*, 2012, **4**(4), 310–316.
34 P. Su, W. Li, C. Zhang, Q. Meng, C. Shen and G. Zhang, Metal based gels as versatile precursors to synthesize stiff and integrated MOF/polymer composite membranes, *J. Mater. Chem. A*, 2015, **3**(40), 20345–20351.
35 A. Y. Al-Maharma, S. P. Patil and B. Markert, Effects of porosity on the mechanical properties of additively manufactured components: a critical review, *Mater. Res. Express*, 2020, **7**(12), 122001.
36 A. Ojuva, M. Järveläinen, M. Bauer, L. Keskinen, M. Valkonen, F. Akhtar, E. Levänen and L. Bergström, Mechanical performance and CO2 uptake of ion-exchanged zeolite A structured by freeze-casting, *J. Eur. Ceram. Soc.*, 2015, **35**(9), 2607–2618.
37 Z. Chen, X. Wang, H. Noh, G. Ayoub, G. W. Peterson, C. T. Buru, T. Islamoglu and O. K. Farha, Scalable, room temperature, and water-based synthesis of functionalized zirconium-based metal–organic frameworks for toxic chemical removal, *CrystEngComm*, 2019, **21**(14), 2409–2415.
38 W. Li, Q. Meng, C. Zhang and G. Zhang, Metal–Organic Framework/PVDF Composite Membranes with High H2 Permselectivity Synthesized by Ammoniation, *Chem. – Eur. J.*, 2015, **21**(19), 7224–7230.
39 H. Zhu, X. Yang, E. D. Cranston and S. Zhu, Flexible and Porous Nanocellulose Aerogels with High Loadings of Metal–Organic-Framework Particles for Separations Applications, *Adv. Mater.*, 2016, **28**(35), 7652–7657.
40 L. Qian, D. Lei, X. Duan, S. Zhang, W. Song, C. Hou and R. Tang, Design and preparation of metal-organic framework papers with enhanced mechanical properties and good antibacterial capacity, *Carbohydr. Polym.*, 2018, **192**, 44–51.
41 S. Palaniandy and N. H. Jamil, Influence of milling conditions on the mechanochemical synthesis of CaTiO3 nanoparticles, *J. Alloys Compd.*, 2009, **476**(1), 894–902.
42 P. A. Thiessen, K. Meyer and G. Heinicke, Grundlagen der Tribochemie, 194 S., 157 Abb., 23 Tab., DIN A 4, 1967 Akademie Verlag, Berlin-Ost, 33,— DM, *Mater. Corros.*, 1968, **19**(2), 188–189.
43 S. Lukin, L. S. Germann, T. Friščić and I. Halasz, Toward Mechanistic Understanding of Mechanochemical Reactions

Using Real-Time In Situ Monitoring, *Acc. Chem. Res.*, 2022, **55**(9), 1262–1277.
44 A. A. L. Michalchuk and F. Emmerling, Time-Resolved In Situ Monitoring of Mechanochemical Reactions, *Angew. Chem., Int. Ed.*, 2022, **61**(21), e202117270.
45 G. Heinicke, *Tribochemistry*, ed. C. Hanser, 1984.
46 T. Friščić, I. Halasz, P. J. Beldon, A. M. Belenguer, F. Adams, S. A. J. Kimber, V. Honkimäki and R. E. Dinnebier, Real-time and in situ monitoring of mechanochemical milling reactions, *Nat. Chem.*, 2013, **5**(1), 66–73.
47 K. Užarević, I. Halasz and T. Friščić, Real-Time and In Situ Monitoring of Mechanochemical Reactions: A New Playground for All Chemists, *J. Phys. Chem. Lett.*, 2015, **6**(20), 4129–4140.
48 C. F. Burmeister and A. Kwade, Process engineering with planetary ball mills, *Chem. Soc. Rev.*, 2013, **42**(18), 7660–7667.
49 M. Toozandehjani, K. A. Matori, F. Ostovan, S. Abdul Aziz and M. S. Mamat, Effect of Milling Time on the Microstructure, Physical and Mechanical Properties of Al-Al2O3 Nanocomposite Synthesized by Ball Milling and Powder Metallurgy, *Materials*, 2017, **10**(11), 1232.
50 G. Jiang, K. Ramachandraiah, Z. Wu, S. Li and J.-B. Eun, Impact of ball-milling time on the physical properties, bioactive compounds, and structural characteristics of onion peel powder, *Food Biosci.*, 2020, **36**, 100630.
51 S. D. Kaloshkin, I. A. Tomilin, G. A. Andrianov, U. V. Baldokhin and E. V. Shelekhov, Phase Transformations and Hyperfine Interactions in Mechanically Alloyed Fe-Cu Solid Solutions, *Mater. Sci. Forum*, 1996, **235–238**, 565–570.
52 L. B. Hong, C. Bansal and B. Fultz, Steady state grain size and thermal stability of nanophase Ni3Fe and Fe3X (X = Si, Zn, Sn) synthesized by ball milling at elevated temperatures, *Nanostruct. Mater.*, 1994, **4**(8), 949–956.
53 N. Cindro, M. Tireli, B. Karadeniz, T. Mrla and K. Užarević, Investigations of Thermally Controlled Mechanochemical Milling Reactions, *ACS Sustainable Chem. Eng.*, 2019, **7**(19), 16301–16309.
54 J. M. Andersen and J. Mack, Decoupling the Arrhenius equation via mechanochemistry, *Chem. Sci.*, 2017, **8**(8), 5447–5453.
55 M. AmanNejad and K. Barani, Effects of Ball Size Distribution and Mill Speed and Their Interactions on Ball Milling Using DEM, *Miner. Process. Extr. Metall. Rev.*, 2021, **42**(6), 374–379.
56 A. Pichon, A. Lazuen-Garay and S. L. James, Solvent-free synthesis of a microporous metal–organic framework, *CrystEngComm*, 2006, **8**(3), 211–214.
57 M. Klimakow, P. Klobes, A. F. Thünemann, K. Rademann and F. Emmerling, Mechanochemical Synthesis of Metal –Organic Frameworks: A Fast and Facile Approach toward Quantitative Yields and High Specific Surface Areas, *Chem. Mater.*, 2010, **22**(18), 5216–5221.
58 M. Y. Masoomi, S. Beheshti and A. Morsali, Mechanosynthesis of new azine-functionalized Zn(ii) metal–organic frameworks for improved catalytic performance, *J. Mater. Chem. A*, 2014, **2**(40), 16863–16866.
59 M. Y. Masoomi, K. C. Stylianou, A. Morsali, P. Retailleau and D. Maspoch, Selective CO2 Capture in Metal–Organic Frameworks with Azine-Functionalized Pores Generated by Mechanosynthesis, *Cryst. Growth Des.*, 2014, **14**(5), 2092–2096.
60 J. Beamish-Cook, K. Shankland, C. A. Murray and P. Vaqueiro, Insights into the Mechanochemical Synthesis of MOF-74, *Cryst. Growth Des.*, 2021, **21**(5), 3047–3055.
61 C. Zhang, Y. Chen, H. Wu, H. Li, X. Li, S. Tu, Z. Qiao, D. An and Q. Xia, Mechanochemical synthesis of a robust cobalt-based metal–organic framework for adsorption separation methane from nitrogen, *Chem. Eng. J.*, 2022, **435**, 133876.
62 N. K. Singh, M. Hardi and V. P. Balema, Mechanochemical synthesis of an yttrium based metal–organic framework, *Chem. Commun.*, 2013, **49**(10), 972–974.
63 A. M. Fidelli, B. Karadeniz, A. J. Howarth, I. Huskić, L. S. Germann, I. Halasz, M. Etter, S.-Y. Moon, R. E. Dinnebier, V. Stilinović, O. K. Farha, T. Friščić and K. Užarević, Green and rapid mechanosynthesis of high-porosity NU- and UiO-type metal–organic frameworks, *Chem. Commun.*, 2018, **54**(51), 6999–7002.
64 M. Rautenberg, B. Bhattacharya, C. Das and F. Emmerling, Mechanochemical Synthesis of Phosphonate-Based Proton Conducting Metal–Organic Frameworks, *Inorg. Chem.*, 2022, **61**(28), 10801–10809.
65 M. Rautenberg, M. Gernhard, J. Radnik, J. Witt, C. Roth and F. Emmerling, Mechanochemical Synthesis of Fluorine-Containing Co-Doped Zeolitic Imidazolate Frameworks for Producing Electrocatalysts, *Front. Chem.*, 2022, **10**, 840758.
66 B. Yi, H. Zhao, L. Cao, X. Si, Y. Jiang, P. Cheng, Y. Zuo, Y. Zhang, L. Su, Y. Wang, C. K. Tsung, L. Y. Chou and J. Xie, A direct mechanochemical conversion of Pt-doped metal-organic framework-74 from doped metal oxides for CO oxidation, *Mater. Today Nano*, 2022, **17**, 100158.
67 M. F. Thorne, M. L. R. Gómez, A. M. Bumstead, S. Li and T. D. Bennett, Mechanochemical synthesis of mixed metal, mixed linker, glass-forming metal–organic frameworks, *Green Chem.*, 2020, **22**(8), 2505–2512.
68 S. Tanaka, T. Nagaoka, A. Yasuyoshi, Y. Hasegawa and J. F. M. Denayer, Hierarchical Pore Development of ZIF-8 MOF by Simple Salt-Assisted Mechanosynthesis, *Cryst. Growth Des.*, 2018, **18**(1), 274–279.
69 K. Imawaka, M. Sugita, T. Takewaki and S. Tanaka, Mechanochemical synthesis of bimetallic CoZn-ZIFs with sodalite structure, *Polyhedron*, 2019, **158**, 290–295.
70 J. Cheng, K. Liu, X. Li, L. Huang, J. Liang, G. Zheng and G. Shan, Nickel-metal-organic framework nanobelt based composite membranes for efficient Sr2+ removal from aqueous solution, *Environ. Sci. Ecotechnology*, 2020, **3**, 100035.
71 J. Cheng, J. Liang, L. Dong, J. Chai, N. Zhao, S. Ullah, H. Wang, D. Zhang, S. Imtiaz, G. Shan and G. Zheng, Self-assembly of 2D-metal–organic framework/graphene oxide membranes as highly efficient adsorbents for the removal of Cs+ from aqueous solutions, *RSC Adv.*, 2018, **8**(71), 40813–40822.

72 P. Zhang, H. Li, G. M. Veith and S. Dai, Soluble Porous Coordination Polymers by Mechanochemistry: From Metal-Containing Films/Membranes to Active Catalysts for Aerobic Oxidation, *Adv. Mater.*, 2015, **27**(2), 234–239.
73 O. Barreda, G. R. Lorzing and E. D. Bloch, Mechanochemical synthesis of two-dimensional metal-organic frameworks, *Powder Diffr.*, 2019, **34**(2), 119–123.
74 J. Hafizović, A. Krivokapić, K. C. Szeto, S. Jakobsen, K. P. Lillerud, U. Olsbye and M. Tilset, Tailoring the Dimensionality of Metal–Organic Frameworks Incorporating Pt and Pd. From Molecular Complexes to 3D Networks, *Cryst. Growth Des.*, 2007, **7**(11), 2302–2304.
75 J. Liang, X. Li, R. Xi, G. Shan, P.-Z. Li, J. Liu, Y. Zhao and R. Zou, A Robust Aluminum Metal-Organic Framework with Temperature-Induced Breathing Effect, *ACS Mater. Lett.*, 2020, **2**(3), 220–226.
76 M. Y. B. Zulkifli, Y. Yao, R. Chen, M. Chai, K. Su, X. Li, Y. Zhou, R. Lin, Z. Zhu, K. Liang, V. Chen and J. Hou, Phase control of ZIF-7 nanoparticles via mechanochemical synthesis, *Chem. Commun.*, 2022, **58**(88), 12297–12300.
77 H. Jeong and J. Lee, 3D-Superstructured Networks Comprising Fe-MIL-88A Metal-Organic Frameworks Under Mechanochemical Conditions, *Eur. J. Inorg. Chem.*, 2019, **2019**(42), 4597–4600.
78 A. Karmakar, M. S. Dodd, X. Zhang, M. S. Oakley, M. Klobukowski and V. K. Michaelis, Mechanochemical synthesis of 0D and 3D cesium lead mixed halide perovskites, *Chem. Commun.*, 2019, **55**(35), 5079–5082.
79 T. D. Bennett, S. Cao, J. C. Tan, D. A. Keen, E. G. Bithell, P. J. Beldon, T. Friscic and A. K. Cheetham, Facile Mechanosynthesis of Amorphous Zeolitic Imidazolate Frameworks, *J. Am. Chem. Soc.*, 2011, **133**(37), 14546–14549.
80 T. Panda, S. Horike, K. Hagi, N. Ogiwara, K. Kadota, T. Itakura, M. Tsujimoto and S. Kitagawa, Mechanical Alloying of Metal–Organic Frameworks, *Angew. Chem., Int. Ed.*, 2017, **56**(9), 2413–2417.
81 S. Cao, T. D. Bennett, D. A. Keen, A. L. Goodwin and A. K. Cheetham, Amorphization of the prototypical zeolitic imidazolate framework ZIF-8 by ball-milling, *Chem. Commun.*, 2012, **48**(63), 7805–7807.
82 M. F. Thorne, A. F. Sapnik, L. N. McHugh, A. M. Bumstead, C. Castillo-Blas, D. S. Keeble, M. Diaz Lopez, P. A. Chater, D. A. Keen and T. D. Bennett, Glassy behaviour of mechanically amorphised ZIF-62 isomorphs, *Chem. Commun.*, 2021, **57**(73), 9272–9275.
83 A. R. Yavari, P. J. Desré and T. Benameur, Mechanically driven alloying of immiscible elements, *Phys. Rev. Lett.*, 1992, **68**(14), 2235–2238.
84 C. Gente, M. Oehring and R. Bormann, Formation of thermodynamically unstable solid solutions in the Cu-Co system by mechanical alloying, *Phys. Rev. B*, 1993, **48**(18), 13244–13252.
85 K. Için, S. ÖZtÜRk, D. D. ÇAkil and S. E. SÜNbÜL, Mechanochemical synthesis of SrFe12O19 from recycled mill scale: Effect of synthesis time on phase formation and magnetic properties, *J. Alloys Compd.*, 2021, **873**, 159787.
86 K. Liang, R. Ricco, C. M. Doherty, M. J. Styles, S. Bell, N. Kirby, S. Mudie, D. Haylock, A. J. Hill, C. J. Doonan and P. Falcaro, Biomimetic mineralization of metal-organic frameworks as protective coatings for biomacromolecules, *Nat. Commun.*, 2015, **6**(1), 7240.
87 T.-T. Chen, J.-T. Yi, Y.-Y. Zhao and X. Chu, Biomineralized Metal–Organic Framework Nanoparticles Enable Intracellular Delivery and Endo-Lysosomal Release of Native Active Proteins, *J. Am. Chem. Soc.*, 2018, **140**(31), 9912–9920.
88 S. K. Alsaiari, S. Patil, M. Alyami, K. O. Alamoudi, F. A. Aleisa, J. S. Merzaban, M. Li and N. M. Khashab, Endosomal Escape and Delivery of CRISPR/Cas9 Genome Editing Machinery Enabled by Nanoscale Zeolitic Imidazolate Framework, *J. Am. Chem. Soc.*, 2018, **140**(1), 143–146.
89 W. Liang, H. Xu, F. Carraro, N. K. Maddigan, Q. Li, S. G. Bell, D. M. Huang, A. Tarzia, M. B. Solomon, H. Amenitsch, L. Vaccari, C. J. Sumby, P. Falcaro and C. J. Doonan, Enhanced Activity of Enzymes Encapsulated in Hydrophilic Metal–Organic Frameworks, *J. Am. Chem. Soc.*, 2019, **141**(6), 2348–2355.
90 S. Gao, J. Hou, Z. Deng, T. Wang, S. Beyer, A. G. Buzanich, J. J. Richardson, A. Rawal, R. Seidel, M. Y. Zulkifli, W. Li, T. D. Bennett, A. K. Cheetham, K. Liang and V. Chen, Improving the Acidic Stability of Zeolitic Imidazolate Frameworks by Biofunctional Molecules, *Chem*, 2019, **5**(6), 1597–1608.
91 P. Horcajada, C. Serre, M. Vallet-Regí, M. Sebban, F. Taulelle and G. Férey, Metal–Organic Frameworks as Efficient Materials for Drug Delivery, *Angew. Chem., Int. Ed.*, 2006, **45**(36), 5974–5978.
92 P. Horcajada, C. Serre, G. Maurin, N. A. Ramsahye, F. Balas, M. Vallet-Regí, M. Sebban, F. Taulelle and G. Férey, Flexible Porous Metal-Organic Frameworks for a Controlled Drug Delivery, *J. Am. Chem. Soc.*, 2008, **130**(21), 6774–6780.
93 R. Babarao and J. Jiang, Unraveling the Energetics and Dynamics of Ibuprofen in Mesoporous Metal–Organic Frameworks, *J. Phys. Chem. C*, 2009, **113**(42), 18287–18291.
94 E. Boldyreva, Mechanochemistry of inorganic and organic systems: what is similar, what is different?, *Chem. Soc. Rev.*, 2013, **42**(18), 7719–7738.
95 J. Nawrocki, D. Prochowicz, A. Wiśniewski, I. Justyniak, P. Goś and J. Lewiński, Development of an SBU-Based Mechanochemical Approach for Drug-Loaded MOFs, *Eur. J. Inorg. Chem.*, 2020, **2020**(10), 796–800.
96 J. Liang, V. Gvilava, C. Jansen, S. Öztürk, A. Spieß, J. Lin, S. Xing, Y. Sun, H. Wang and C. Janiak, Cucurbituril-Encapsulating Metal–Organic Framework via Mechanochemistry: Adsorbents with Enhanced Performance, *Angew. Chem., Int. Ed.*, 2021, **60**(28), 15365–15370.
97 B. Szczęśniak, J. Phuriragpitikhon, J. Choma and M. Jaroniec, Mechanochemical synthesis of three-component graphene oxide/ordered mesoporous carbon/metal-organic framework composites, *J. Colloid Interface Sci.*, 2020, **577**, 163–172.
98 V. Polshettiwar, J. Thivolle-Cazat, M. Taoufik, F. Stoffelbach, S. Norsic and J.-M. Basset, "Hydro-metathesis" of Olefins: A

Catalytic Reaction Using a Bifunctional Single-Site Tantalum Hydride Catalyst Supported on Fibrous Silica (KCC-1) Nanospheres, *Angew. Chem., Int. Ed.*, 2011, **50**(12), 2747–2751.

99 B. Li, J.-G. Ma and P. Cheng, Integration of Metal Nanoparticles into Metal–Organic Frameworks for Composite Catalysts: Design and Synthetic Strategy, *Small*, 2019, **15**(32), 1804849.

100 T. Ishida, M. Nagaoka, T. Akita and M. Haruta, Deposition of Gold Clusters on Porous Coordination Polymers by Solid Grinding and Their Catalytic Activity in Aerobic Oxidation of Alcohols, *Chem. – Eur. J.*, 2008, **14**(28), 8456–8460.

101 H.-L. Jiang, B. Liu, T. Akita, M. Haruta, H. Sakurai and Q. Xu, Au@ZIF-8: CO Oxidation over Gold Nanoparticles Deposited to Metal–Organic Framework, *J. Am. Chem. Soc.*, 2009, **131**(32), 11302–11303.

102 S. A. Noorian, N. Hemmatinejad and J. A. R. Navarro, Bioactive molecule encapsulation on metal-organic framework via simple mechanochemical method for controlled topical drug delivery systems, *Microporous Mesoporous Mater.*, 2020, **302**, 110199.

103 P. C. Reshmi Varma, Low-Dimensional Perovskites, in *Perovskite Photovoltaics*, ed. S. Thomas and A. Thankappan, Academic Press, 2018, ch. 7, pp. 197–229.

104 X. Lin, H. Su, S. He, Y. Song, Y. Wang, Z. Qin, Y. Wu, X. Yang, Q. Han, J. Fang, Y. Zhang, H. Segawa, M. Grätzel and L. Han, In situ growth of graphene on both sides of a Cu–Ni alloy electrode for perovskite solar cells with improved stability, *Nat. Energy*, 2022, **7**, 520–527.

105 Y. Chen, S. Liu, N. Zhou, N. Li, H. Zhou, L.-D. Sun and C.-H. Yan, An overview of rare earth coupled lead halide perovskite and its application in photovoltaics and light emitting devices, *Prog. Mater. Sci.*, 2021, **120**, 100737.

106 J. Aguilera-Sigalat and D. Bradshaw, Synthesis and applications of metal-organic framework–quantum dot (QD@MOF) composites, *Coord. Chem. Rev.*, 2016, **307**, 267–291.

107 P. D. Sutrisna, J. Hou, H. Li, Y. Zhang and V. Chen, Improved operational stability of Pebax-based gas separation membranes with ZIF-8: a comparative study of flat sheet and composite hollow fibre membranes, *J. Membr. Sci.*, 2017, **524**, 266–279.

108 S. Jin, H.-J. Son, O. K. Farha, G. P. Wiederrecht and J. T. Hupp, Energy Transfer from Quantum Dots to Metal–Organic Frameworks for Enhanced Light Harvesting, *J. Am. Chem. Soc.*, 2013, **135**(3), 955–958.

109 Z. Chen, Z.-G. Gu, W.-Q. Fu, F. Wang and J. Zhang, A Confined Fabrication of Perovskite Quantum Dots in Oriented MOF Thin Film, *ACS Appl. Mater. Interfaces*, 2016, **8**(42), 28737–28742.

110 D. Rambabu, S. Bhattacharyya, T. Singh, C. M. L. and T. K. Maji, Stabilization of $MAPbBr_3$ Perovskite Quantum Dots on Perovskite MOFs by a One-Step Mechanochemical Synthesis, *Inorg. Chem.*, 2020, **59**(2), 1436–1443.

111 N. Khosroshahi, M. Bakhtian and V. Safarifard, Mechanochemical synthesis of ferrite/MOF nanocomposite: Efficient photocatalyst for the removal of meropenem and hexavalent chromium from water, *J. Photochem. Photobiol., A*, 2022, **431**, 114033.

112 S. Wu, G. Zhuang, J. Wei, Z. Zhuang and Y. Yu, Shape control of core–shell MOF@MOF and derived MOF nanocages via ion modulation in a one-pot strategy, *J. Mater. Chem. A*, 2018, **6**(37), 18234–18241.

113 K. A. McDonald, J. I. Feldblyum, K. Koh, A. G. Wong-Foy and A. J. Matzger, Polymer@MOF@MOF: "grafting from" atom transfer radical polymerization for the synthesis of hybrid porous solids, *Chem. Commun.*, 2015, **51**(60), 11994–11996.

114 L. Zhang, J. Wang, X. Ren, W. Zhang, T. Zhang, X. Liu, T. Du, T. Li and J. Wang, Internally extended growth of core–shell NH2-MIL-101(Al)@ZIF-8 nanoflowers for the simultaneous detection and removal of Cu(ii), *J. Mater. Chem. A*, 2018, **6**(42), 21029–21038.

115 Y. Gu, Y.-N. Wu, L. Li, W. Chen, F. Li and S. Kitagawa, Controllable Modular Growth of Hierarchical MOF-on-MOF Architectures, *Angew. Chem., Int. Ed.*, 2017, **56**(49), 15658–15662.

116 J. Hou, C. W. Ashling, S. M. Collins, A. Krajnc, C. Zhou, L. Longley, D. N. Johnstone, P. A. Chater, S. Li, M.-V. Coulet, P. L. Llewellyn, F.-X. Coudert, D. A. Keen, P. A. Midgley, G. Mali, V. Chen and T. D. Bennett, Metal-organic framework crystal-glass composites, *Nat. Commun.*, 2019, **10**(1), 2580.

117 R. Lin, X. Li, A. Krajnc, Z. Li, M. Li, W. Wang, L. Zhuang, S. Smart, Z. Zhu, D. Appadoo, J. R. Harmer, Z. Wang, A. G. Buzanich, S. Beyer, L. Wang, G. Mali, T. D. Bennett, V. Chen and J. Hou, Mechanochemically Synthesised Flexible Electrodes Based on Bimetallic Metal–Organic Framework Glasses for the Oxygen Evolution Reaction, *Angew. Chem., Int. Ed.*, 2022, **61**(4), e202112880.

118 C. Liu, J. Wang, J. Wan, Y. Cheng, R. Huang, C. Zhang, W. Hu, G. Wei and C. Yu, Amorphous Metal–Organic Framework-Dominated Nanocomposites with Both Compositional and Structural Heterogeneity for Oxygen Evolution, *Angew. Chem., Int. Ed.*, 2020, **59**(9), 3630–3637.

119 F. Sun, G. Wang, Y. Ding, C. Wang, B. Yuan and Y. Lin, NiFe-Based Metal–Organic Framework Nanosheets Directly Supported on Nickel Foam Acting as Robust Electrodes for Electrochemical Oxygen Evolution Reaction, *Adv. Energy Mater.*, 2018, **8**(21), 1800584.

120 M. A. Ghanem, A. Basu, R. Behrou, N. Boechler, A. J. Boydston, S. L. Craig, Y. Lin, B. E. Lynde, A. Nelson, H. Shen and D. W. Storti, The role of polymer mechanochemistry in responsive materials and additive manufacturing, *Nat. Rev. Mater.*, 2021, **6**(1), 84–98.

121 A. Krusenbaum, S. Grätz, G. T. Tigineh, L. Borchardt and J. G. Kim, The mechanochemical synthesis of polymers, *Chem. Soc. Rev.*, 2022, **51**(7), 2873–2905.

122 Y. Chen, G. Mellot, D. van Luijk, C. Creton and R. P. Sijbesma, Mechanochemical tools for polymer materials, *Chem. Soc. Rev.*, 2021, **50**(6), 4100–4140.

123 D. Chen, J. Zhao, P. Zhang and S. Dai, Mechanochemical synthesis of metal–organic frameworks, *Polyhedron*, 2019, **162**, 59–64.

124 N. S. Punde, C. R. Rawool, A. S. Rajpurohit, S. P. Karna and A. K. Srivastava, Hybrid Composite Based on Porous Cobalt-Benzenetricarboxylic Acid Metal Organic Framework and Graphene Nanosheets as High Performance Supercapacitor Electrode, *ChemistrySelect*, 2018, **3**(41), 11368–11380.

125 Q.-X. Luo, M. Ji, M.-H. Lu, C. Hao, J.-S. Qiu and Y.-Q. Li, Organic electron-rich N-heterocyclic compound as a chemical bridge: building a Brönsted acidic ionic liquid confined in MIL-101 nanocages, *J. Mater. Chem. A*, 2013, **1**(22), 6530–6534.

126 V. Lykourinou, Y. Chen, X.-S. Wang, L. Meng, T. Hoang, L.-J. Ming, R. L. Musselman and S. Ma, Immobilization of MP-11 into a Mesoporous Metal–Organic Framework, MP-11@mesoMOF: A New Platform for Enzymatic Catalysis, *J. Am. Chem. Soc.*, 2011, **133**(27), 10382–10385.

127 P. Manna, J. Debgupta, S. Bose and S. K. Das, A Mononuclear CoII Coordination Complex Locked in a Confined Space and Acting as an Electrochemical Water-Oxidation Catalyst: A "Ship-in-a-Bottle" Approach, *Angew. Chem., Int. Ed.*, 2016, **55**(7), 2425–2430.

128 Y. Sun, H. Huang, H. Vardhan, B. Aguila, C. Zhong, J. A. Perman, A. M. Al-Enizi, A. Nafady and S. Ma, Facile Approach to Graft Ionic Liquid into MOF for Improving the Efficiency of CO2 Chemical Fixation, *ACS Appl. Mater. Interfaces*, 2018, **10**(32), 27124–27130.

129 Q.-L. Zhu and Q. Xu, Metal–organic framework composites, *Chem. Soc. Rev.*, 2014, **43**(16), 5468–5512.

130 T. Ishida, N. Kawakita, T. Akita and M. Haruta, One-potN-alkylation of primary amines to secondary amines by gold clusters supported on porous coordination polymers, *Gold Bull.*, 2009, **42**(4), 267–274.

131 H.-L. Jiang, Q.-P. Lin, T. Akita, B. Liu, H. Ohashi, H. Oji, T. Honma, T. Takei, M. Haruta and Q. Xu, Ultrafine Gold Clusters Incorporated into a Metal–Organic Framework, *Chem. – Eur. J.*, 2011, **17**(1), 78–81.

132 C. Orellana-Tavra, R. J. Marshall, E. F. Baxter, I. A. Lázaro, A. Tao, A. K. Cheetham, R. S. Forgan and D. Fairen-Jimenez, Drug delivery and controlled release from biocompatible metal–organic frameworks using mechanical amorphization, *J. Mater. Chem. B*, 2016, **4**(47), 7697–7707.

133 Y. Sun, X. Jia, H. Huang, X. Guo, Z. Qiao and C. Zhong, Solvent-free mechanochemical route for the construction of ionic liquid and mixed-metal MOF composites for synergistic CO2 fixation, *J. Mater. Chem. A*, 2020, **8**(6), 3180–3185.

134 J. Oktawiec, H. Z. H. Jiang, J. G. Vitillo, D. A. Reed, L. E. Darago, B. A. Trump, V. Bernales, H. Li, K. A. Colwell, H. Furukawa, C. M. Brown, L. Gagliardi and J. R. Long, Negative cooperativity upon hydrogen bond-stabilized O2 adsorption in a redox-active metal–organic framework, *Nat. Commun.*, 2020, **11**(1), 3087.

135 M. Parsaei, E. Roudbari, F. Piri, A. S. El-Shafay, C.-H. Su, H. C. Nguyen, M. Alashwal, S. Ghazali and M. Algarni, Neural-based modeling adsorption capacity of metal organic framework materials with application in wastewater treatment, *Sci. Rep.*, 2022, **12**(1), 4125.

136 R. Ou, H. Zhang, V. X. Truong, L. Zhang, H. M. Hegab, L. Han, J. Hou, X. Zhang, A. Deletic, L. Jiang, G. P. Simon and H. Wang, A sunlight-responsive metal–organic framework system for sustainable water desalination, *Nat. Sustain.*, 2020, **3**(12), 1052–1058.

137 M. Bonneau, C. Lavenn, J.-J. Zheng, A. Legrand, T. Ogawa, K. Sugimoto, F.-X. Coudert, R. Reau, S. Sakaki, K.-I. Otake and S. Kitagawa, Tunable acetylene sorption by flexible catenated metal–organic frameworks, *Nat. Chem.*, 2022, **14**, 816–822.

138 B. Levasseur, C. Petit and T. J. Bandosz, Reactive Adsorption of NO2 on Copper-Based Metal–Organic Framework and Graphite Oxide/Metal–Organic Framework Composites, *ACS Appl. Mater. Interfaces*, 2010, **2**(12), 3606–3613.

139 J. Park, Y. S. Chae, D. W. Kang, M. Kang, J. H. Choe, S. Kim, J. Y. Kim, Y. W. Jeong and C. S. Hong, Shaping of a Metal–Organic Framework–Polymer Composite and Its CO2 Adsorption Performances from Humid Indoor Air, *ACS Appl. Mater. Interfaces*, 2021, **13**(21), 25421–25427.

140 T. Saeed, A. Naeem, I. U. Din, M. Farooq, I. W. Khan, M. Hamayun and T. Malik, Synthesis of chitosan composite of metal-organic framework for the adsorption of dyes; kinetic and thermodynamic approach, *J. Hazard. Mater.*, 2022, **427**, 127902.

141 Y. Sun, M. Chen, H. Liu, Y. Zhu, D. Wang and M. Yan, Adsorptive removal of dye and antibiotic from water with functionalized zirconium-based metal organic framework and graphene oxide composite nanomaterial Uio-66-(OH)2/GO, *Appl. Surf. Sci.*, 2020, **525**, 146614.

142 M. Sarker, J. Y. Song and S. H. Jhung, Adsorptive removal of anti-inflammatory drugs from water using graphene oxide/metal-organic framework composites, *Chem. Eng. J.*, 2018, **335**, 74–81.

143 P. Liu, T. Zhao, K. Cai, P. Chen, F. Liu and D.-J. Tao, Rapid mechanochemical construction of HKUST-1 with enhancing water stability by hybrid ligands assembly strategy for efficient adsorption of SF6, *Chem. Eng. J.*, 2022, **437**, 135364.

144 G. Liu, H. Chen, W. Zhang, Q. Ding, J. Wang and L. Zhang, Facile mechanochemistry synthesis of magnetic covalent organic framework composites for efficient extraction of microcystins in lake water samples, *Anal. Chim. Acta*, 2021, **1166**, 338539.

145 L. Wang, X. Feng, L. Ren, Q. Piao, J. Zhong, Y. Wang, H. Li, Y. Chen and B. Wang, Flexible Solid-State Supercapacitor Based on a Metal–Organic Framework Interwoven by Electrochemically-Deposited PANI, *J. Am. Chem. Soc.*, 2015, **137**(15), 4920–4923.

146 T. Wei, M. Zhang, P. Wu, Y.-J. Tang, S.-L. Li, F.-C. Shen, X.-L. Wang, X.-P. Zhou and Y.-Q. Lan, POM-based metal-organic framework/reduced graphene oxide nanocomposites with hybrid behavior of battery-supercapacitor for superior lithium storage, *Nano Energy*, 2017, **34**, 205–214.

147 J. Yang, F. Zhang, H. Lu, X. Hong, H. Jiang, Y. Wu and Y. Li, Hollow Zn/Co ZIF Particles Derived from Core–Shell ZIF-67@ZIF-8 as Selective Catalyst for the Semi-Hydrogenation

of Acetylene, *Angew. Chem., Int. Ed.*, 2015, **54**(37), 10889–10893.

148 B. Liu, H. Shioyama, H. Jiang, X. Zhang and Q. Xu, Metal–organic framework (MOF) as a template for syntheses of nanoporous carbons as electrode materials for supercapacitor, *Carbon*, 2010, **48**(2), 456–463.

149 K. W. Chapman, D. F. Sava, G. J. Halder, P. J. Chupas and T. M. Nenoff, Trapping Guests within a Nanoporous Metal–Organic Framework through Pressure-Induced Amorphization, *J. Am. Chem. Soc.*, 2011, **133**(46), 18583–18585.

150 X. Xu, R. Cao, S. Jeong and J. Cho, Spindle-like Mesoporous α-Fe2O3 Anode Material Prepared from MOF Template for High-Rate Lithium Batteries, *Nano Lett.*, 2012, **12**(9), 4988–4991.

151 Y. Han, P. Qi, X. Feng, S. Li, X. Fu, H. Li, Y. Chen, J. Zhou, X. Li and B. Wang, In Situ Growth of MOFs on the Surface of Si Nanoparticles for Highly Efficient Lithium Storage: Si@MOF Nanocomposites as Anode Materials for Lithium-Ion Batteries, *ACS Appl. Mater. Interfaces*, 2015, **7**(4), 2178–2182.

152 B. L. Souza, S. Chauque, P. F. M. de Oliveira, F. F. Emmerling and R. M. Torresi, Mechanochemical optimization of ZIF-8/Carbon/S8 composites for lithium-sulfur batteries positive electrodes, *J. Electroanal. Chem.*, 2021, **896**, 115459.

153 L. Chen, S. Deng, H. Liu, J. Wu, H. Qi and J. Chen, Giant energy-storage density with ultrahigh efficiency in lead-free relaxors via high-entropy design, *Nat. Commun.*, 2022, **13**(1), 3089.

154 F.-M. Zhang, L.-Z. Dong, J.-S. Qin, W. Guan, J. Liu, S.-L. Li, M. Lu, Y.-Q. Lan, Z.-M. Su and H.-C. Zhou, Effect of Imidazole Arrangements on Proton-Conductivity in Metal–Organic Frameworks, *J. Am. Chem. Soc.*, 2017, **139**(17), 6183–6189.

155 J. Y. Kim, R. Balderas-Xicohténcatl, L. Zhang, S. G. Kang, M. Hirscher, H. Oh and H. R. Moon, Exploiting Diffusion Barrier and Chemical Affinity of Metal–Organic Frameworks for Efficient Hydrogen Isotope Separation, *J. Am. Chem. Soc.*, 2017, **139**(42), 15135–15141.

156 S. Liu, Z. Yue and Y. Liu, Incorporation of imidazole within the metal–organic framework UiO-67 for enhanced anhydrous proton conductivity, *Dalton Trans.*, 2015, **44**(29), 12976–12980.

157 Z. Lin, L. Li, L. Yu, W. Li and G. Yang, Dual-functional photocatalysis for hydrogen evolution from industrial wastewaters, *Phys. Chem. Chem. Phys.*, 2017, **19**(12), 8356–8362.

158 S. Garcia-Segura and E. Brillas, Applied photoelectrocatalysis on the degradation of organic pollutants in wastewaters, *J. Photochem. Photobiol., C*, 2017, **31**, 1–35.

159 V. Glembockyte, M. Frenette, C. Mottillo, A. M. Durantini, J. Gostick, V. Štrukil, T. Friščić and G. Cosa, Highly Photostable and Fluorescent Microporous Solids Prepared via Solid-State Entrapment of Boron Dipyrromethene Dyes in a Nascent Metal–Organic Framework, *J. Am. Chem. Soc.*, 2018, **140**(49), 16882–16887.

160 L. Protesescu, S. Yakunin, M. I. Bodnarchuk, F. Krieg, R. Caputo, C. H. Hendon, R. X. Yang, A. Walsh and M. V. Kovalenko, Nanocrystals of Cesium Lead Halide Perovskites (CsPbX3, X = Cl, Br, and I): Novel Optoelectronic Materials Showing Bright Emission with Wide Color Gamut, *Nano Lett.*, 2015, **15**(6), 3692–3696.

161 J. Zhang, Z. Zhao, Z. Xia and L. Dai, A metal-free bifunctional electrocatalyst for oxygen reduction and oxygen evolution reactions, *Nat. Nanotechnol.*, 2015, **10**(5), 444–452.